NAVAL POSTGRADUATE SCHOOL

MONTEREY, CALIFORNIA

THESIS

SENSITIVITY ANALYSIS OF THE SEAKEEPING BEHAVIOR OF TRIMARAN SHIPS

by

Aziz Alper Kurultay

December 2003

Thesis Advisor: Fotis Papoulias

Approved for public release; distribution is unlimited

THIS PAGE INTENTIONALLY LEFT BLANK

REPORT DOCUMENTATION PAGE			Form Approved OMB No. 0704-0188
Public reporting burden for this collection of information is estimated to average 1 hour per response, including the time for reviewing instruction, searching existing data sources, gathering and maintaining the data needed, and completing and reviewing the collection of information. Send comments regarding this burden estimate or any other aspect of this collection of information, including suggestions for reducing this burden, to Washington headquarters Services, Directorate for Information Operations and Reports, 1215 Jefferson Davis Highway, Suite 1204, Arlington, VA 22202-4302, and to the Office of Management and Budget, Paperwork Reduction Project (0704-0188) Washington DC 20503.			
1. AGENCY USE ONLY *(Leave blank)*	**2. REPORT DATE** December 2003	**3. REPORT TYPE AND DATES COVERED** Master's Thesis	
4. TITLE AND SUBTITLE: Sensitivity Analysis of the Seakeeping Behavior of Trimaran Ships			**5. FUNDING NUMBERS**
6. AUTHOR(S) Aziz A. Kurultay			
7. PERFORMING ORGANIZATION NAME(S) AND ADDRESS(ES) Naval Postgraduate School Monterey, CA 93943-5000			**8. PERFORMING ORGANIZATION REPORT NUMBER**
9. SPONSORING /MONITORING AGENCY NAME(S) AND ADDRESS(ES) N/A			**10. SPONSORING/MONITORING AGENCY REPORT NUMBER**
11. SUPPLEMENTARY NOTES The views expressed in this thesis are those of the author and do not reflect the official policy or position of the Department of Defense or the U.S. Government.			
12a. DISTRIBUTION / AVAILABILITY STATEMENT Approved for public release; distribution is unlimited.			**12b. DISTRIBUTION CODE**

13. ABSTRACT (maximum 200 words)

The dynamic response of the ship while operating in different sea conditions is one of the design parameters of a hull form. The objective of this thesis is to analyze the seakeeping response of trimaran hulls. A three-dimensional Rankine source panel method is used to achieve that. Seakeeping response characteristics of a typical trimaran with a variable separation ratio (the ratio of the lateral distance between center hull and side hull to the length of the ship) and with different longitudinal positions of the side hulls are analyzed. Heave and pitch motion response amplitude operators are evaluated for bow, bow quartering, and beam waves in irregular seas at various ship forward speeds. The corresponding heave and pitch responses were calculated by applying the Bretschneider spectral formulation. Seakeeping behaviors of the generic trimaran are classified based on the plots of root mean square values for every position of the side hulls at different sea states in to determine optimal location of the side hulls with regards to seakeeping

14. SUBJECT TERMS Seakeeping, Ship Response Spectrum, Trimaran Hull Form, SWAN2, Root Mean Square, Response Amplitude Operator			**15. NUMBER OF PAGES** 87
			16. PRICE CODE
17. SECURITY CLASSIFICATION OF REPORT Unclassified	**18. SECURITY CLASSIFICATION OF THIS PAGE** Unclassified	**19. SECURITY CLASSIFICATION OF ABSTRACT** Unclassified	**20. LIMITATION OF ABSTRACT** UL

NSN 7540-01-280-5500

Standard Form 298 (Rev. 2-89)
Prescribed by ANSI Std. 239-18

THIS PAGE INTENTIONALLY LEFT BLANK

Approved for public release; distribution is unlimited

SENSITIVITY ANALYSIS OF THE SEAKEEPING BEHAVIOR OF TRIMARAN SHIPS

Aziz A. Kurultay
Lieutenant Junior Grade, Turkish Navy
B.S., Turkish Naval Academy, 1998

Submitted in partial fulfillment of the
requirements for the degree of

MASTER OF SCIENCE IN MECHANICAL ENGINEERING

from the

NAVAL POSTGRADUATE SCHOOL
December 2003

Author: Aziz A. Kurultay

Approved by: Fotis A. Papoulias
Thesis Advisor

Anthony J. Healey
Chairman, Department of Mechanical and Astronautical Engineering

THIS PAGE INTENTIONALLY LEFT BLANK

ABSTRACT

The dynamic response of the ship while operating in different sea conditions is one of the design parameters of a hull form. The objective of this thesis is to analyze the seakeeping response of trimaran hulls. A three-dimensional Rankine source panel method is used to achieve that. Seakeeping response characteristics of a typical trimaran with a variable separation ratio (the ratio of the lateral distance between center hull and side hull to the length of the ship) and with different longitudinal positions of the side hulls are analyzed. Heave and pitch motion response amplitude operators are evaluated for bow, bow quartering, and beam waves in irregular seas at various ship forward speeds. The corresponding heave and pitch responses were calculated by applying the Bretschneider spectral formulation. Seakeeping behaviors of the generic trimaran are classified based on the plots of root mean square values for every position of the side hulls at different sea states in to determine optimal location of the side hulls with regards to seakeeping.

THIS PAGE INTENTIONALLY LEFT BLANK

TABLE OF CONTENTS

LIST OF FIGURES

LIST OF TABLES

THIS PAGE INTENTIONALLY LEFT BLANK

ACKNOWLEDGMENTS

I would like to thank all of the people who supported me through this great opportunity and challenging endeavor at Naval Postgraduate School. I would like to thank my family, for their loving support over all the years of my education. Feeling their support from thousands of miles away gave me courage to succeed. Without values of hard work and determination that my parents instilled in me, I would not be able to take on such challenges as these.

I would like to thank my thesis advisor, Professor Fotis Papoulias both for my thesis work and for Total Ship Systems Engineering experience. His vision and technical expertise in the field of naval architecture and control systems made this thesis work possible.

Finally, I would like to dedicate my thesis work my parents, Akin and Ayten Kurultay. They have given me all their love and support throughout my education.

THIS PAGE INTENTIONALLY LEFT BLANK

I. INTRODUCTION

It is recognized throughout the ship design community that seakeeping (i.e., the response of a ship in a seaway) is an important parameter in ship design. As a result, there have been many studies on the seakeeping behavior of surface ships. Most of these studies, however, are for traditional monohulls ships. The main reason for this is that monohulls have dominated ship design practice for centuries. As more modern missions emerge, multihull ships have emerged as a practical alternative considering their variety of advantages. It is important, therefore, to conduct a series of studies on the seakeeping behavior of multihulls in order to gain some insight that could be utilized in the design process.

Chapter II of this thesis presents a literature review of hull forms and a summary of their advantages and disadvantages with regards to their seakeeping. Particular emphasis is placed on the trimaran hull form which is the basis for the current study. Multihull ships present a particular difficulty in the analysis process, namely interaction between the hulls. For traditional monohulls, a simplifying assumption is often made: Hydrodynamic characteristics are calculated for two dimensional sections of the hull and then integrated throughout the length. This is called *strip theory* and has the obvious advantage of reducing a three dimensional problem into a series of two dimensional problems. This approach will not work for multihull ships. Hydrodynamic interactions between the hulls cast a high degree of 3-D effects into the problem, which cannot be analyzed adequately by strip theory. Furthermore, in a two dimensional setting, one may observe generation of standing waves between the hulls, which are not present in the true 3-D problem. Therefore, a tool other than strip theory is necessary in this problem.

Chapter III presents a summary of the hydrodynamic problem, and Chapter IV its numerical implementation using SWAN, the analysis tool that we followed in this work. SWAN is a three dimensional code based on panel methods. Panels are distributed throughout the surface of the ship and the free surface. Source strength is evaluated by satisfying the boundary conditions. 368 Simulation runs were made at three different wave headings, at four different ship forward speeds, and three positions in lateral direction, ten positions in longitudinal direction of the side hulls in order to evaluate

Response Amplitude Operators (RAOs) in irregular seas. Results from the sensitivity analysis runs are presented in Chapter V, along with some conclusions and recommendations for further research.

.

II. MOTIVATION

A. LITERATURE REVIEW ON HULL FORMS

In this chapter, conventional monohulls and non-conventional advanced hull forms are reviewed by identifying the evolving requirements for the Navy. The basic advantages and disadvantages of these hull forms are outlined. Finally, some of the trimaran hull form's outstanding benefits are reviewed based on some recent studies.

Two major influences have affected conventional hull forms in the formation of ship design. The first dramatic change resulted as a shift from blue water (open ocean) focus to operation in littoral environments, especially in the United States Navy, which resulted from a need to counter new threats. These new threats include land-based enemy forces as well as small crafts, mines and other shallow water threats, [1] According to *High Speed, Small Naval Vessel Technology Development Plan* in 2003, high speed ship missions require 40-60 knots for ship designs, but with extensive experience designing and building monohulls, the U.S. shipbuilding industry is still not able to reach these speed limits utilizing conventional monohulls. One example of the current state of the art for high speed ship design is 72 m Swedish corvette KNM Visby. This 650 tons gas turbine ship has a maximum speed of 38 knots.

The second influence is Expeditionary Warfare. According to *Monohull, Catamaran, Trimaran and SES High Speed Sealift Vessels*, there is a time gap between transferring the first forces by airlift and bringing in the heavier supporting equipment via traditional sealift. This time gap necessitates High Speed Sealift, [2]. Defining strategic sealift as the target mission requires ship designs to achieve 50-60 knots service speeds in long ocean transit sea states, [3]. Payloads varied from a few hundred tons for the least demanding intra-theater mission to 12,000 tons for the most demanding inter-theater missions. On the other hand, reliable development of slower traditional monohulls has been achieved over many decades. This capability has been displayed for displacements over 40,000 tons and speeds approaching 40 knots (SS United States). Even with enormous design experience on monohulls is still not sufficient to meet the needs of the High Speed Sealift.

These evolving requirements have generated new design needs for the Navy and have forced designers to surpass the shortcomings of the conventional monohulls. It should be noted that monohulls have been the most widely used hull forms due to their extensive advantages; less power requirements for long distances at low speeds; efficient use of enclosed volume; robustness, viability and durability; tolerance to weight and displacement growth; and cost efficiency. Despite these advantages, monohulls display some weaknesses in a variety of design aspects.

The relatively large waterplane area of monohulls, an advantage when considering weight growth, is a negative factor when considering the issue of seakeeping especially in head seas and beam seas. Although it is a great simplification, it can be said that a ship will react to the dynamic input of swells and waves proportional to the waterplane area and that an increased area will result in more intense ship motions.

Monohulls have other shortcomings like small deck area and unfavorable lateral stability characteristics, particularly for high-performance slender monohulls. This hull form is also characterized by limited speed and by sensitivity to slamming, spraying of green water, and degraded performance in developed seaways due to large pitch and roll motions and high accelerations.

Achieving the speed and range requirements identified for naval monohulls requires significantly more slender hulls than traditional designs. But slenderness and high speed also have definite effects on performance and structural design. Low structural weight is a design priority that can be achievable by increased slenderness, but high speeds will likely result in significant slam loads in Sea State 5 or worse conditions. [3] Hull girders for hydrodynamically slender hulls are also structurally slender. As a result, structural loads and reactions to the loads such as slam induced whipping, both vertical and lateral, are expected to have critical importance for slender high speed monohulls. [3] The resulting high-frequency, large amplitude accelerations are expected to have significant effects on hull fatigue life, crew, cargo and payload.

The above limitations have led to the development of the following non-monohull forms, which generally offer higher speed potential and greater stability in certain operating conditions than conventional monohulls.

Besides monohulls, other displacement crafts like catamarans, trimarans, and SWATHs depend largely on buoyancy support. By utilizing power lift (ACV, SES) or dynamic lift (hydrofoil), advanced hull forms can provide higher speeds by reducing or nearly eliminating either the wave-making resistance or the hull surface frictional resistance. Also they can provide better stability at higher speeds than monohulls as well as better seakeeping performance in severe sea states. Of course, each non-conventional hull form design has its operational disadvantages which limit its suitability to certain missions.

1. Catamaran

Catamarans are characterized by two slender hulls, connected by a common deck and a center bow. The role of this center bow is to reduce the incidence of slamming for head seas by decreasing damping. This multihull form takes advantage of shallow draft, larger deck areas, and higher propulsion efficiencies. Catamarans provide better seakeeping and maneuverability than monohulls afforded by slender, widely separated hulls and propulsion.

There is a number of appealing design alternatives within the catamaran category. One of them is the wave-piercing catamaran, a design exclusively built by *INCAT Australia Pty Ltd.* This design features side hulls with a very low freeboard at their bows and a definite, above-water center bow. Additional hull separation of this configuration provides some benefits in terms of seakeeping in short-period waves and the extra reserve buoyancy derived from the centre hull, which is undoubtedly of benefit in more significant sea conditions. Clearly their hull form and slenderness ratios make them particularly efficient at high speed.

According to Sea Trials of *Joint Venture HSV-X1 by The Naval Warfare Development Command (NWDC)* as the ship pitches into the waves, the buoyancy provided by the immersion of the centre bow causes the ship to reduce its pitching motion. Even though forces associated with bow immersion can have large magnitudes in heavy sea conditions, these forces are distributed all through the longitudinal structural load path. [4]

Although catamarans are more widely held as commercial ferries in restricted or coastal waters, their seakeeping performance is not as good as SES and SWATH, which limit their potential for blue water operations.

2. SWATH (Small Waterplane Area Twin Hull)

The design concept of SWATH ships consists of two hulls submerged beneath the water's surface, which connect to the upper hulls by thin single or tandem struts.

The chief attribute of SWATH is its seakeeping performance. The flexibility of SWATH geometry allows a selection of hull forms having natural periods which shift ship responses away from wave frequencies likely to be encountered. SWATH vessels are characterized by small waterplane areas and relatively long natural periods of motion. If the natural periods of a ship are substantially longer than the prevailing ocean waves, the ship will experience little motion especially at low speeds. SWATH configurations provide the most feasible means of obtaining desired long heave, pitch, and roll periods in a relatively small ship. In addition to having better seakeeping performance than similar monohulls, a SWATH is able to maintain speed in high sea states because of the amelioration of slamming.

The Stena HSS line ferries and Danyard/NQEA Seajet crafts are of this arrangement and exhibit significantly improved motion characteristics compared to conventional catamaran hull forms.[1] However, conventional SWATH hulls suffer from powering inefficiencies at higher speeds, excessive draft and sensitivity to weight loading/unloading. Therefore, this hull form has been limited to wide-area survey or surveillance operations. [4]

3. Sea Slice

SLICE hull form utilizes four short hulls, in which the forward pair is fitted with propulsors, instead of the SWATH's two long hulls. This hull form has been developed by *Lockheed Martin NE&SS-Marine Systems* under the sponsorship of *Office on Naval Research (ONR).*

SLICE offers not only the advantages of a conventional SWATH vessel in terms of seakeeping and stability, but also provides a high cruise speed at relatively low powers. This is accomplished through reducing wave making drag, using short struts and

operating beyond the hump on the Froude resistance curve, [5]. Also the SLICE form affords significant propulsion, displacement, and hydrodynamic efficiencies compared to conventional SWATH design according to *Lockheed Martin NE&SS-Marine Systems*. Construction of Sea SLICE, used to validate the performance of the SLICE hull form, was enabled under an agreement between *Lockheed Martin* and *ONR*. [4]

4. SES (Surface Effect Ship)

This concept uses very slender vertical catamaran-style side hulls to enclose the two sides of the air cushion and utilizes the flexible skirt at the bow and the stern area. When air cushion pressure raises the vessel, its side hulls remain slightly immersed to contain air cushion. The side hulls enhance the underway maneuverability and stability of the SES.

According to Umoe Mandal AS, advantages of this concept are shallow draft and low resistance in the air cushion mode, higher speeds than conventional monohulls, better seakeeping characteristics. In the off cushion mode, resistance increases significantly and maneuverability advantage diminishes like superior seakeeping performance.

Royal Norwegian Navy's fast missile patrol craft *KNM Skjold*, a 154 foot composite ship, uses an Air Cushion Catamaran (ACC) design, which is an advanced variant of SES technology. Most recently, a co-operative design team that includes the naval design firm of *J.J. Mcmullen & Assoc., Atlantic Marine, Goodrich* and *Umoe Mandal* and led by *Raytheon* has proposed a SES vessel design based on the Norwegian *KNM Skjold* as its preliminary bid for the Littoral Combat Ship design contract, [6].

5. Hydrofoils

The hydrofoil hull form supports itself by lift force generated by water passing around under water foils after certain speed. At foilborne speeds, the hull of the craft can be lifted out of water completely, but at lower speeds it uses only buoyant lift. Higher speeds can be obtained by changing the angle of attack of foils. Two foil systems are used for hydrofoil craft. First, surface piercing V-shaped or U-shaped foils and second, fully submerged foils. The benefit of this hull form is fuel efficiency at high speed due to reduced resistance.

However, at a deeper draft several disadvantages are obvious, namely ineffectiveness when operating slowly, and vulnerability to damage. Cavitation and ventilation problems around foils are other disadvantages. As a consequence, hydrofoil ships have been limited to small to medium capacity commercial ferries and fast patrol boats, which have about 500 tons in displacement.

6. Hybrids

Hybrid hull forms utilize two or all three basic forces, which are buoyant lift, dynamic lift and powered lift. A noteworthy hybrid is an adaptation of SES vessel *IX 515* so-called Hybrid Small Waterplane Area Craft (HYSWAC). *Nigel Gee and Associates* has provided detail and structural design for this modification.

HYSWAC uses dynamic lift generated by hydrofoils to supplement buoyant lift. According to the company the key advantages of the vessel are; much less roll, heave, and pitch compared with a monohull, high-damping efficiency at low-to-zero speeds, and better hydrodynamic efficiency than monohull above 20 knots, reduced resistance and power hump compared with pure hydrofoil vessels. But excessive draft of this modified hull form limits its usage, [4].

B. ADVANTAGES OF TRIMARAN HULL FORMS

A trimaran hull form consists of long slender main hull and two relatively small sidehulls. Many research papers are available that investigated the advantages of large trimaran configurations for future cargo ships and alternative frigate/destroyer size warships. There are also several trimaran designs being investigated, which claim both high speed and high hull efficiency. The key benefits of trimaran can be summarized in different design considerations.

1. Seakeeping

According to *The General Dynamics Bath Iron Works* spokesman, the overall seakeeping responses are significant compare to conventional monohull. The long, slender waterline of the main hull provides better seakeeping performance especially head and bow quartering seas by reducing heave and pitch motion. This is caused by the increase in length to displacement ratio of the main hull. The lateral stability of this hull form is similar to monohull at small heel angles and similar to catamaran at larger heel angles because of the improved lateral stability characteristic due to twin sidehulls. [4]

One of the weaknesses of monohulls is the rolling performance in the beam seas as mentioned. This situation is turned out to be a significant attraction of trimarans. The major influence on the roll motion is the value of metacentric height (GM). With the same GM as a monohull, the roll natural frequency of a trimaran tends to be less than the monohull because of its greater beam and roll inertia and tends to see lower roll acceleration.

The other influence on heave, roll, and pitch motions is the amount of damping in the form of appendages such as bilge keels and foils. In this respect, the breadth of trimarans provides an opportunity for using foil type dampers attached to the sidehulls. The foils have significant effects on motions due to the damping contribution of an appendage is proportional to the cube of the distance from the radius of gyration. [7]

2. Resistance, Propulsion, Maneuverability

The slender hull form, with its two sidehulls, reduces drag at high speeds by 20 percent compared to an equivalent monohull design. The trimaran's lower resistance at operational speeds permits reduction in the size of propulsion plant, which also leads to lower life-cycle cost and fuel consumption.

Trimaran offers layout benefits of propulsion plant installation. Propulsion plant can be split evenly between the sidehulls with nothing in the main hull; located in the main hull only; or divided between the main hull and sidehulls in various proportions. Podded propulsion can be used in trimarans effectively; specifically installation of the propulsors in the sidehulls can increase maneuverability. Another possibility for main hull propulsion is waterjet for high speed ships, and if steerable they have the additional benefit of better low speed maneuverability. [8]

3. Deck Area and Growth Margin

By the positioning of the sidehulls, up to 40 percent increase in deck area can be achievable compared to similar monohull. This increase offers more space for hangars, helicopter operation and enclosed volume for weapon systems. Consequently, large deck area improves effectiveness of the whole ship design.

The trimaran hull form provides greater top weight growth margin. The area of growth margin increases lateral stability significantly. This growth margin allows equipment upgrades during life cycle of the ship.

4. Additional Advantages

The trimaran hull form has stealth potential to reduce radar cross section and infrared signature. Reduction in heat signature could be gained by exhausting between the sidehulls rather than conventional main structure funneling.

Equipment could be mounted higher on the ship so the effect of the shock levels could be reduced. This arrangement decreases the likelihood of the equipment failures in operations.

According to spokesman of the *Vosper Thornycroft (VT) Shipyard*, the sidehull increase the ability to mount sensors higher above the waterline to improve early-warning missile defense capabilities. Also the sidehulls could be utilized for configuring multi-line towed array sonar, [8], [9].

These advantages make trimaran hull form preliminary candidate for future warships. The *RV Triton* is one product of these challenges. This ship is the largest steel trimaran ever built. Co-operative research efforts and trials between *U.K. Defense Evaluation and Research Agency* and *U.S. Navy's Office of Naval Research* are still undergoing. According to *Sea Power International* magazine, the *RV Triton* has been described as one of the most significant developments in warship design. [10]

III. MODELING BACKGROUND

A. THEORETICAL APPROACH

1. Problem Definition

For potential flow computations the fluid is assumed to be inviscid, homogeneous and incompressible. Surface tension on the free surface is neglected. Figure 1 displays a ship advancing with a time dependent forward speed U(t) in ambient waves. The Cartesian coordinate system x=(x,y,z) is fixed on the ship and is translating with velocity U(t) in the positive x-direction. The ambient waves are propagating toward the ship with an absolute frequency ω creating angle β with the x-direction. (β=180° means bow waves)

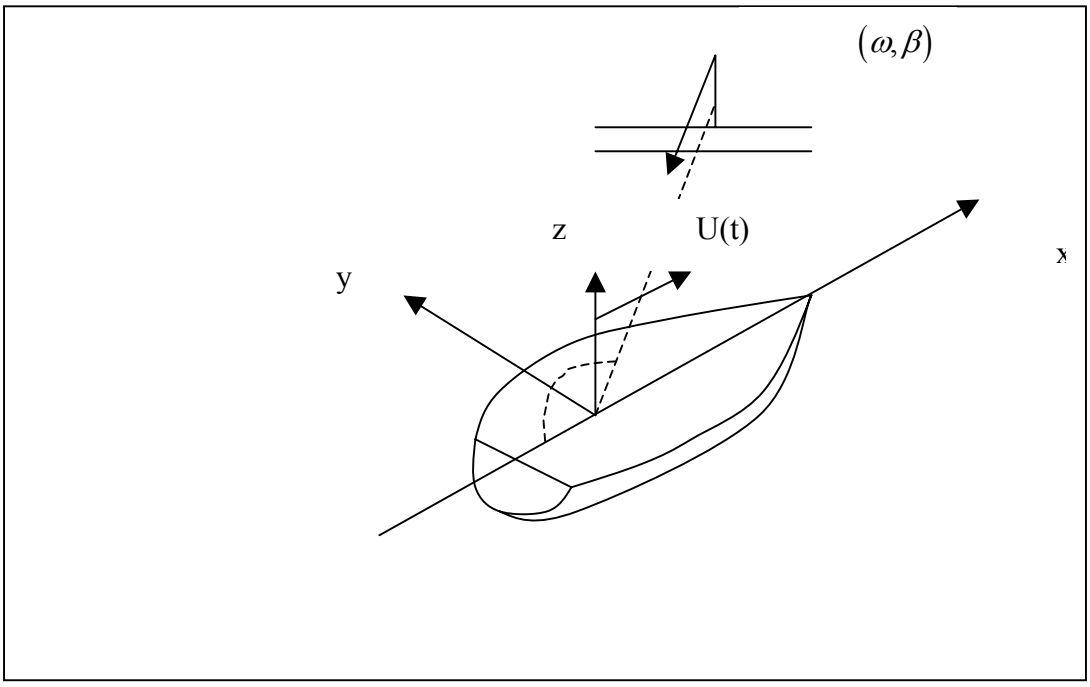

Figure 1. Coordinate system U(t)

A ship with forward speed U (t) starts to move from rest at $t = 0$. The fluid is at rest at t<0 and for t>0 the fluid disturbance starts to develop from three different sources:

i) The trim and sinkage displacement of the ship around its mean calm water position.

ii) The steady motion of the ship with forward speed U around its mean calm water position.

iii) The interaction of the ship with incident waves, [11].

The disturbance fluid velocity $v(x,t)$ is defined as the gradient of the velocity potential $\Phi(x,t)$, or $v=\nabla\Phi$ assuming potential flow. Φ is subject to the Laplace equation in the fluid domain because of continuity.

$$\nabla^2\Phi \equiv \frac{\partial^2\Phi}{\partial x^2}+\frac{\partial^2\Phi}{\partial y^2}+\frac{\partial^2\Phi}{\partial z^2}=0 \tag{3.1}$$

The position of the free surface is defined by the wave elevation $\zeta(x,y,t)$ in addition to the velocity potential $\Phi(x,t)$. They are the pair of unknown quantities, or namely state variables.

State variables are related to each other by two conditions on the free surface, kinematic and dynamic conditions. The kinematic condition requires that a fluid particle on the air-water interface at rest $t=0$ will be stationary all the times. The corresponding mathematical expression relative to the translating reference takes this form,

$$\left[\frac{\partial}{\partial t}-(\vec{U}-\nabla\Phi)\bullet\nabla\right]\zeta=\frac{\partial\Phi}{\partial z} \text{ on z=}\zeta(x,y,t) \tag{3.2}$$

The dynamic condition basically states that the fluid pressure on the free surface and the atmospheric pressure must be equal. Bernoulli's equation can be written for the dynamic condition as follows

$$\left[\frac{\partial}{\partial t}-\vec{U}\bullet\nabla\right]\Phi+\frac{1}{2}\nabla\Phi\bullet\nabla\Phi=-g\zeta \text{ on z=}\zeta(x,y,t) \tag{3.3}$$

A more compact free surface condition, which involves the velocity potential explicitly and the wave elevation implicitly can be obtained by eliminating the wave elevation ζ from (3.2) and (3.3).

The flow normal velocity equals the corresponding the rigid boundary velocity on the ship hull. The unit vector normal to the instantaneous position of the ship hull is denoted by **n**, and

$$\frac{\partial \Phi}{\partial n} = \vec{U} \bullet \vec{n} + \vec{v} \bullet \vec{n} \tag{3.4}$$

where $\vec{v}$ is the oscillatory velocity potential of the ship hull caused by the wave induced motions. The flow velocity must disappear at large distances from the ship at any given finite time, [12].

2. Linearization of Free Surface Conditions

For the linearization of the free surface conditions to be justified two conditions must hold. The first one requires the wave slope to be small and the second one requires the hull shape to be sufficiently 'streamlined', namely thin, slender or flat. The most important consequence of the previous assumption is that the fluid disturbance velocity due to the ship forward translation and its oscillatory motion in waves are both small compared to its speed U. As a result of this, the total velocity potential Φ may be divided into two parts, the basis-flow potential φ_0 and the disturbance-flow potential φ_1, [12]. These potentials are defined as follows

$$\Phi = \varphi_0 + \varphi_1 \text{ where } \left|\nabla \varphi_1\right| \ll \left|\nabla \varphi_0\right| \tag{3.5}$$

A similar decomposition is applied for the wave elevation ζ,

$$\zeta = \zeta_0 + \zeta_1 \text{ where } \zeta_1 \ll \zeta_0 \tag{3.6}$$

The Neumann-Kelvin linearization is the simplest linearization method and assumes that the basis flow is the uniform stream. The corresponding basis wave elevation is zero and the resulting free surface condition for the two state variables take the following form,

$$\left(\frac{\partial}{\partial t} - U\frac{\partial}{\partial x}\right)\zeta_1 = \frac{\partial \varphi_1}{\partial z} \text{ on z=0} \tag{3.7}$$

$$\left(\frac{\partial}{\partial t} - U\frac{\partial}{\partial x}\right)\varphi_1 = -g\zeta_1 \text{ on z=0} \tag{3.8}$$

The Neumann-Kelvin model has limitations; it can be justified only for ships that have vanishing small beam or draft. A more accurate basis-flow model exists for conventional ships with finite beam and draft of comparable magnitude, and this model accounts for the effects of the ship thickness.

In the Double-Linearization method, the flow past the ship and its positive image above the free surface may be selected as the basis flow. For this reason, this linearization is referred to the double-body flow, [13]. The effects of the ship thickness are better modeled by the basis flow potential φ_0 over the ship hull. This is the main advantage of this choice over the uniform stream

The resulting basis wave elevation ζ_0 follows Bernoulli's equation (3.3) and takes this form

$$\zeta_0 = \frac{U}{g}\frac{\partial \varphi_0}{\partial x} - \frac{1}{2g}\nabla\varphi_0 \bullet \nabla\varphi_0 \text{ on z=0} \tag{3.9}$$

Using the linearization assumptions and substituting in the nonlinear free-surface conditions leads to the following conditions for (φ_1, ζ_1) over the $z = 0$ plane;

$$\left[\frac{\partial}{\partial t} - \left(\vec{U} - \nabla\varphi_0\right)\bullet\nabla\right]\zeta_1 = \frac{\partial^2\varphi_0}{\partial z^2}\zeta_1 + \frac{\partial\varphi_1}{\partial z} \text{ on z=0} \tag{3.10}$$

$$\left[\frac{\partial}{\partial t} - \left(\vec{U} - \nabla\varphi_0\right)\bullet\nabla\right]\varphi_1 = -g\zeta_1 + \left[\vec{U}\bullet\nabla\varphi_0 - \frac{1}{2}\nabla\varphi_0\bullet\nabla\varphi_0\right] \text{ on z=0} \tag{3.11}$$

According to the *Computation of Wave Ship Interactions* by *Sclavounos (1996)*, *Dawson (1977)* [13] first implemented Double-Body Linearization in a Rankine Panel Method, [12].

3. Linearization of Body Boundary Conditions

The ship undergoes an oscillatory motion with displacements denoted by $\xi_j(t)$, j=1,…,6 in each of its six degrees of freedom in the presence of ambient waves. Surge (j=1), sway (j=2), heave (j=3), roll (j=4), pitch (j=5), yaw (j=6). By assuming that ship's oscillatory displacement is small, the linearization of the exact body boundary condition entails its statement over the mean translating position of the ship hull.

After adopting the decomposition of the total velocity potential Φ into basis and disturbance components, φ_0 and φ_1, the basis potential offsets the normal flux caused by the forward translation of the ship, or

$$\frac{\partial \varphi_0}{\partial n} = \vec{U} \bullet \vec{n} = U n_1 \text{ on } \overline{S} \tag{3.12}$$

where $\mathbf{n}=(n_1, n_2, n_3)$ is the unit vector normal to the ship hull and points out of the fluid domain. The disturbance potential φ_1 consists of incident, diffraction and radiation components and can be decomposed into components in the following form

$$\varphi_1 = \sum_{j=1}^{6} \varphi_{R_j} + \varphi_D + \varphi_I \tag{3.13}$$

where φ_{R_j} are radiation wave potentials corresponding to the $j-th$ mode, φ_D is the diffraction potential and φ_I is the incident potential. All potentials defined above satisfy free surface conditions (3.10) and (3.11) due to linearity. The body boundary conditions on the ship hull are subject to

$$\vec{n} \bullet \nabla \varphi_D \equiv \frac{\partial \varphi_D}{\partial n} = -\frac{\partial \varphi_I}{\partial n} \text{ on } \overline{S} \tag{3.14}$$

The corresponding body boundary condition for the radiation disturbance potential is more complex and takes the form

$$\frac{\partial \varphi_{R_j}}{\partial n} = \sum_{j=1}^{6} \left(\frac{\partial \xi_j}{\partial t} n_j + \xi_j m_j \right) \text{ on } \overline{S} \tag{3.15}$$

where

$$\vec{n} = (n_1, n_2, n_3) \tag{3.16}$$

$$\vec{x} \times \vec{n} = (n_4, n_5, n_6) \tag{3.17}$$

$$(m_1, m_2, m_3) = (\vec{n} \bullet \nabla)\left(\vec{U} - \nabla \varphi_0\right) \tag{3.18}$$

$$(m_4, m_5, m_6) = (\vec{n} \bullet \nabla)\left[\vec{x} \times \left(\vec{U} - \nabla \varphi_0\right)\right] \tag{3.19}$$

The m-terms, m_j, provide a coupling between the steady basis flow and the unsteady body motion.

In the double-body linearization case, the basis flow is modeled by the double-body flow potential. Mentioned model satisfies the exact boundary condition over the ship hull caused by its forward translation and a rigid lid condition on the $z = 0$ plane. This basis flow model leads to a more accurate set of body boundary conditions. [12]

4. Panel Method

Panel methods provide a highly accurate methodology for solving flows past arbitrarily shaped bodies in both two and three dimensions.

The basic idea of panel methods is subdividing the body surface into N flat quadrilaterals using a source distribution over which the source strength are assumed constant. The body boundary conditions at the center of each quadrilateral (also called a node, control, or collocation point) are satisfied and a system of N linear equations for the unknown source strengths is evaluated. The velocity and pressure at each control point can easily be determined by knowing the source strength. Higher order panel methods involve the use of panels that are not flat and/or singularity distribution strengths that are not constant over a panel.

Two tasks require almost all of the computational effort in panel methods. The first is setting up the influence matrix, which requires multiple evaluations of the Green function for the problem. The second is solving the resulting linear system of equations. [14]

a. Rankine Panel Method

A Rankine Panel Method is presented for the solution of the complete three-dimensional steady and time-harmonic potential flows past ships advancing with a forward velocity. A new free surface condition is derived using the linearization about the double-body flow and this is valid uniformly from low to high Froude numbers, [15].The unknown basis potential or disturbance potential is denoted by φ in order to be determined over the mean translating position of the ship hull, S_B, and over the free surface, S_F, which is $z = 0$ plane.[12] The Laplace Equation (3.1) in the fluid domain

bounded by S_B and S_F may be enforced by an application of Green's Theorem for the Rankine source potential and the velocity potential $\varphi(x)$

$$G(\vec{x},\vec{\xi}) = \frac{1}{2\pi\left|\vec{x}-\vec{\xi}\right|} \tag{3.20}$$

Green's identity leads to an integral relation between the velocity potential and the normal derivative of φ over S_B and S_F. Thus, Green's identity becomes

$$\varphi(\vec{x},t) + \iint_{S_F+S_B} \varphi\left(\vec{\xi},t\right)\frac{\partial G}{\partial n_\xi}\left(\vec{x},\vec{\xi}\right)d\xi - \iint_{S_F+S_B} \frac{\partial\varphi\left(\vec{\xi},t\right)}{\partial n_\xi} G\left(\vec{x},\vec{\xi}\right)d\xi = 0 \tag{3.21}$$

The contribution from a closing surface at infinity disappears caused by the decay of $\varphi(x)$ and $G\left(x,\xi\right)$, as $x \to \infty$ for fixed values of ξ.

The normal velocity potential φ_n is known and supplied by the body boundary conditions over S_B. The linearized free surface conditions (3.10) and (3.11) relate $\varphi_n = \varphi_z$ to the value and tangential gradients of φ and ζ over S_F. Substituting these boundary conditions reduces (3.21) into two integro-differential equations for φ over S_B and $\left(\varphi,\zeta\right)$ over S_F. These equations are solved by panel method described in the next chapter. [12]

B. SHIP RESPONSE IN SEA WAVES

1. Plane Progressive Wave

The simplest free surface wave formation, which has great practical significance, is the plane progressive wave system. This motion is two dimensional, sinusoidal in time with angular frequency, and propagates with phase velocity c_p such that to an observer moving this velocity the wave appears to be stationary. [16]

The parameter

$$k = \frac{\omega}{c_p} \tag{3.22}$$

is the wave number, the number of waves per unit distance along the x-axis. Or

$$k = \frac{2\pi}{\lambda} \tag{3.23}$$

where the wavelength λ is the distance between successive points on the wave with the same phase. An additional relation between the wave number k and the frequency ω can be obtained. This relation is called dispersion relation

$$k = \frac{\omega^2}{g} \tag{3.24}$$

Alternatively, the frequency ω can be replaced by the wave period $T = 2\pi / \omega$, just as the wave number k can be replaced by the wavelength $\lambda = 2\pi / k$.

The phase velocity c_p can be determined from (3.21), and using (3.23). It follows that

$$c_p = \frac{\omega}{k} = \frac{g}{\omega} = \sqrt{\frac{g}{k}} = \sqrt{\frac{g\lambda}{2\pi}} \tag{3.25}$$

The last equation states that surface waves in deep water are dispersive, longer waves travel faster than short waves. And the dispersion relation is now

$$k \tan kH = \frac{\omega^2}{g} \tag{3.26}$$

where H is sea bottom depth. It should be noted that as $H \to \infty$ $\tanh kH \to 1$. Therefore, for deep water, dispersion relation takes this form

$$\omega^2 = gk \tag{3.27}$$

The propagating wave has amplitude, has sinusoidal motion with angular frequency and it moves with phase velocity. The wave elevation can be described in the following form

$$\zeta(x, y, t) = A \bullet \Re\left\{\exp\left[-ik\left(x\cos\beta + y\sin\beta\right) + i\omega t\right]\right\} \tag{3.28}$$

where A is the wave amplitude, β is the wave direction relative to the x-axis. [17] In the most general case of a continuous distribution, a two dimensional integral representation follows of the form

$$\zeta(x,y,t) = \Re\int_0^{\infty} d\omega \int_0^{2\pi} d\beta A(\omega,\beta)\exp\left[-ik\left(x\cos\beta + y\sin\beta\right) + i\omega t\right] \qquad (3.29)$$

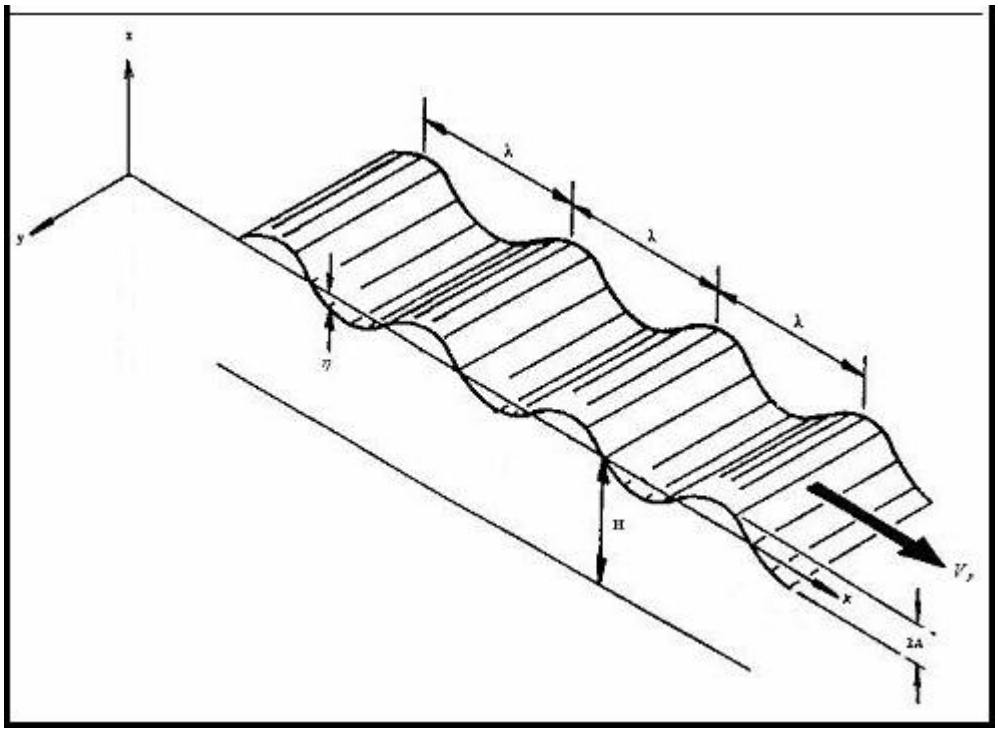

Figure 2. Plane progressive waves (From Ref. [18])

2. Ship Wave System

The most general wave distribution in three dimensions is given by the double integral (3.29). If this is transformed to a reference system moving with the ship in the positive x-direction with steady velocity U, the appropriate expression with x replaced by $x+Ut$ is given by

$$\zeta\left(x,y,t\right) = \Re\int_0^{\infty} d\omega \int_0^{2\pi} d\beta A(\omega,\beta)\exp\left[-ik\left(x\cos\beta + y\sin\beta\right) + i\left(\omega - kU\cos\beta\right)t\right] \qquad (3.30)$$

where $k(\omega)$ is the wave number corresponding to a given frequency ω in accordance with the dispersion relation (3.24) for infinite depth.

If the ship motion is steady state in the reference system that moves with the ship, the previous expression must be independent of time. So the second exponential term disappears,

$$kU\cos\beta-\omega=0 \tag{3.31}$$

which means that phase velocity of each amplitude wave component is given by

$$c_p=\frac{\omega}{k}=U\cos\beta \tag{3.32}$$

By applying equation (3.31) to eliminate one of the variables of integration (3.30), this integration for a steady wake pattern behind the ship takes the following single integral form

$$\zeta(x,y)=\Re\int_{-\pi/2}^{\pi/2}d\beta A(\beta)\exp\left[-ik(\beta)\left(x\cos\beta+y\sin\beta\right)\right] \tag{3.33}$$

This expression is known as the free wave distribution of a given ship. If the distance downstream from the position of the ship is large (far field), the integral (3.33) can be simplified and the classical ship wave pattern can be obtained as derived by *Kelvin* in 1887. [16]

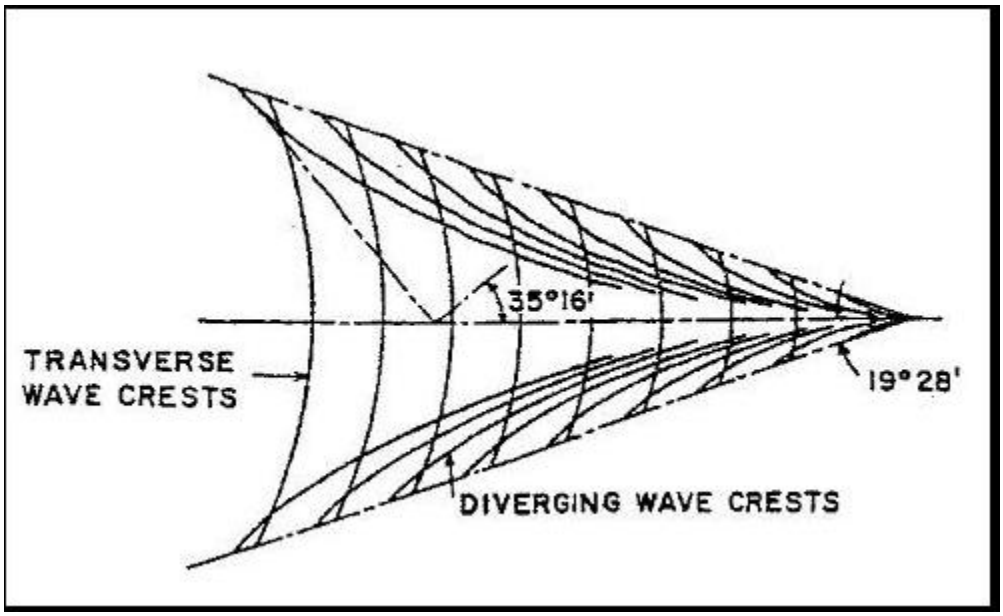

Figure 3. The Kelvin ship wave system (From Ref [16])

The waves in the wake of the ship are limited to a symmetrical sector about the negative x-axis, with included semi angles of $19^{\circ}28'$. The waves on the x-axis move in the same direction as the ship when $\beta=0$ (following seas). The angle of these transverse waves changes while the lateral coordinate y is increased. They reach a value of $\pm35^{\circ}$ on

the boundaries. Larger values of β correspond to diverging waves; these have shorter wavelength and converge towards the origin as shown in Figure 3, [17].

3. Motions in Seaway

The easiest way to discuss the ship motions at sea waves is to assume regular, sinusoidal type, small amplitude type waves. Actual ocean waves are highly irregular but by utilizing the principal of linear superposition this process can be simplified. The principal of superposition states that the response of a ship to an irregular sea can be presented by a linear summation of its responses to the elements of the regular waves that comprise the irregular sea. [19]

The total mean energy of the wave system per unit area of the free surface is in this form

$$\overline{E} = \rho g \int_0^\infty \int_0^{2\pi} S(\omega, \beta) d\beta d\omega \tag{3.34}$$

ρg term can be ignored and the function $S(\omega, \beta)$ is referred as the spectral energy density or simply energy spectrum, and this is unidirectional. It can be integrated over all directions to evaluate frequency spectrum. [16] This wave spectrum is the time history of the wave height, and represents the distribution of energy as a function of wave frequency, with units of $m^2 - \sec$ or $ft^2 - \sec$.

$$S(\omega) = \int_0^{2\pi} S(\omega, \beta) d\beta \tag{3.35}$$

Figure 4 represents typical wave spectrum, which is a statistical illustration of its components.

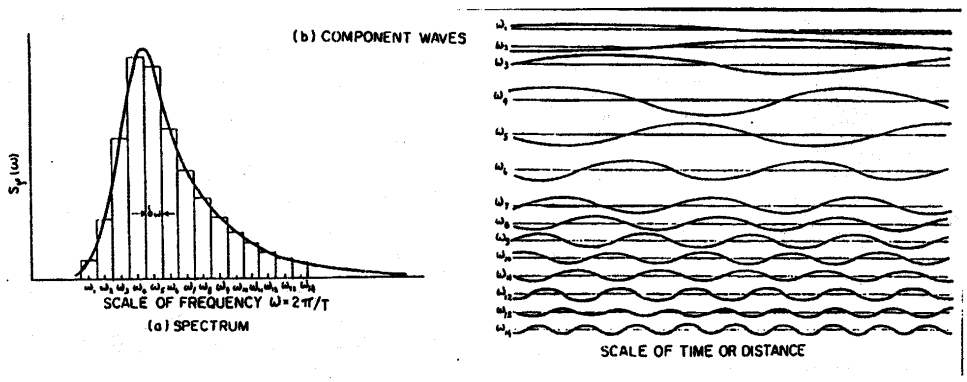

Figure 4. Typical wave spectrum (From Ref.[17])

Figure 5 represents wave spectrum for three different modal periods (T_m) with significant wave height of 1.88m, which is associated with sea state 4. [20] Significant wave height $H_{1/3}$ is defined as the mean of the one third highest waves.

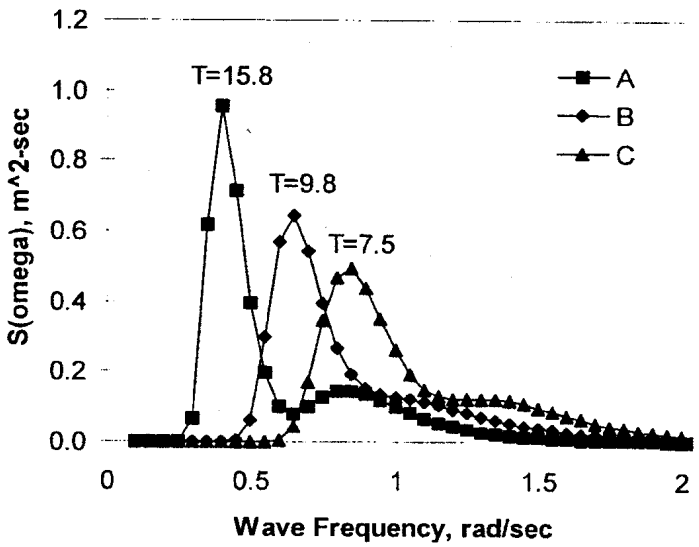

Figure 5. Wave Spectrum for 1.88m (Sea State 4) (From Ref [20])

The peaks are associated with the maximum energy in the wave spectrum. If it is desired to obtain the wave amplitudes A_j the equation takes this form

$$\frac{1}{2}A_j^2 = S\left(\omega_j\right)\Delta\omega_j \quad \text{j=1,2,…,6} \tag{3.36}$$

The total energy of the spectrum, or in other words the integral of $S(\omega)$ over all frequencies is denoted as m_0. In general, the moments m_i of the spectrum are defined by

$$m_i = \int_0^\infty \omega^i S(\omega) d\omega \quad \text{i=0,1,2,…} \tag{3.37}$$

The encounter frequency is the frequency, ω_e, that a moving ship with a forward speed U 'feels'.[16] The encounter frequency is different than absolute frequency, ω. For bow seas $\beta = 180^\circ$ and for the following seas $\beta = 0^\circ$, see Figure 1. The encounter frequency is in this form

$$\omega_e = \omega - \frac{\omega^2}{g} U \cos\beta = \omega - kU\cos\beta \tag{3.38}$$

4. Bretschneider Spectral Formulation

There are many ways to model a wave spectrum. Two of the most common methods are the Pierson-Moskowitz and Bretschneider spectrums. This spectrum is based on analysis of spectral data in the open ocean in the North Atlantic and it was recommended for using by the 15^{th} International Towing Tank Conference (ITTC). The Bretschneider wave spectrum utilizes the modal period inputs based on the information provided by The Spectral Ocean Wave Model (SOWM). SWOM is a hind cast mathematical model which uses wind data to generate of ocean waves in deep water. [20] Table 1 shows the relationship between significant wave height and modal period to Sea States based on the SOWM database.

Sea State	Specific Wave Height (m)	Modal Period Range (sec)	Most Probable Modal Period (sec)	Sustained Wind Speed (kts)
0-1	0-0.1	-	-	0-6
2	0.1-0.5	3.3-12.8	7.5	7-10
3	0.5-1.25	5.0-14.8	7.5	11-16
4	1.25-2.5	6.1-15.2	8.8	17-21
5	2.5-4.0	8.3-15.5	9.7	22-27

6	4.0-6.0	9.8-16.2	12.4	28-47
7	6.0-9.0	11.8-18.5	15.0	48-55
8	9.0-14.0	14.2-18.6	16.4	56-63
>8	>14.0	15.7-23.7	20.0	>63

Table 1. North Atlantic Sea State Table

It's usual to use statistics from the North Atlantic when geographic location is not specified for the ship design purposes. The "Most Probable Modal Period" column presents the modal period associated with the center frequency of the modal period band which has the highest probability of occurrence. [20]

This formulation is a function of both modal frequency and significant wave height and can represent wide range of single peaked wave spectra. And it's convenient to use Bretschneider wave spectral formulation by applying the SOWM databases in seakeeping calculations. [20] In this analysis, the most probable modal periods were utilized to evaluate wave spectrum at each sea state. Bretschneider formulation is

$$S(\omega) = \left(\frac{1.25}{4}\right)\left(\frac{\omega_m{}^4}{\omega^5}\right) H_{1/3}{}^2 \bullet e^{\left[-1.25\left(\frac{\omega_m}{\omega}\right)^4\right]} \tag{3.39}$$

In Figure 6 $S(\omega)$ is plotted for 2 m. significant wave height for a range of modal periods. (Sea State 4)

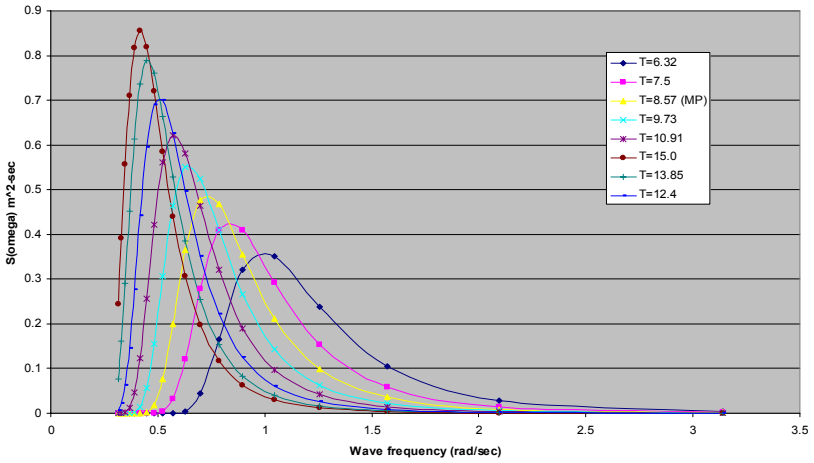

Figure 6. Bretschneider Wave Spectrum for Sea State 4

5. Response Spectra

A ship has six degrees of freedom. Three translational motions: surge, sway, heave and three rotational motions: roll, pitch, and yaw. Figure 7 shows the degrees of freedom and incident wave direction.

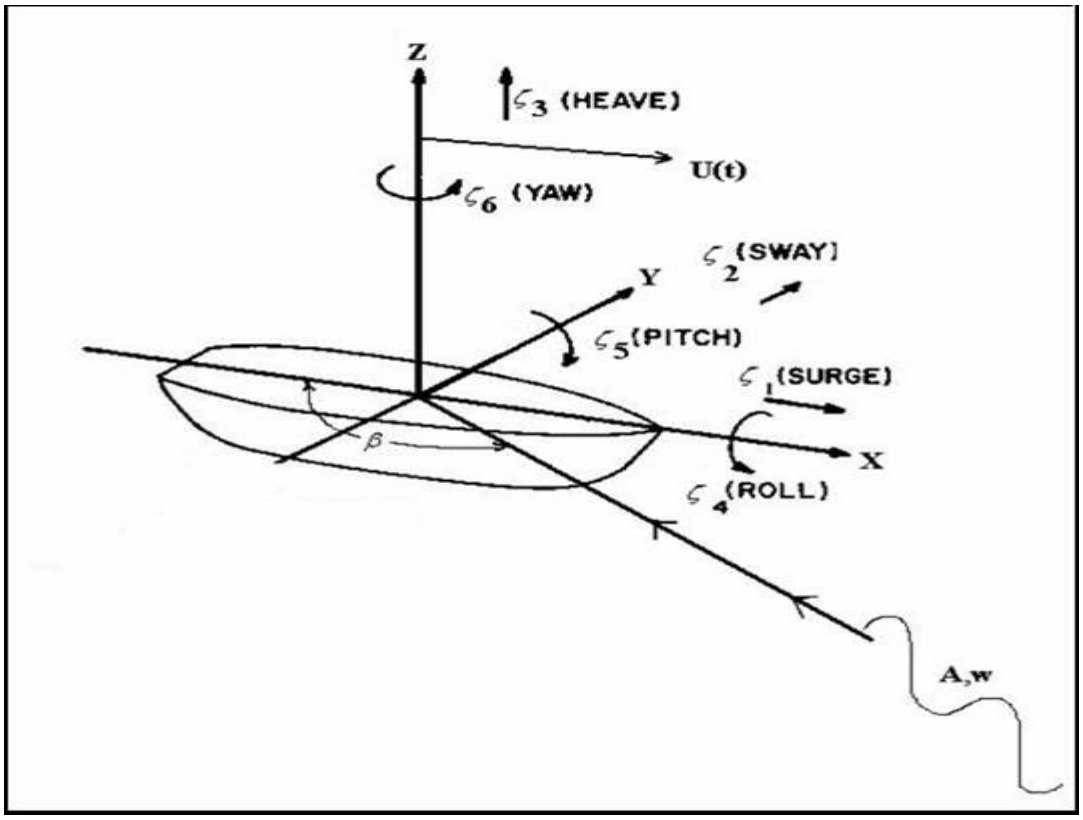

Figure 7. Ship motions, incident wave and six degrees of freedom

First of all the Response Amplitude Operators (RAO) should be evaluated to obtain ship response spectrum. A response amplitude operator is a measure of the ship response to a regular wave of unit amplitude. It should be noted that translational motions are dimensionless (m/m), but rotational motions are expressed degrees per meter of degrees per foot (deg/m, deg/ft). Pitch and roll motions are usually expressed in degrees, even though radian measures could be used instead. [18]

Ship response spectrum is a function of response amplitude operator and wave spectrum, which takes this form

$$S_R(\omega) = |RAO|^2 S(\omega) \tag{3.40}$$

For nonzero forward speeds, ship response spectrum is using the encounter frequency. The encounter frequency represents the Doppler shift of the frequency of the incoming waves as seen from the moving ship. By combining (3.38) and (3.40)

$$S_R(\omega_e) = |RAO|^2 \, S(\omega) \left(1 - \frac{2\omega}{g} U \cos\beta\right)^{-1} \tag{3.43}$$

Figure 8 shows a typical ship response spectrum by applying heave RAOs (ξ_3) produced by SWAN-2 for a 122.24 m, 2506 metric ton trimaran at Froude Number 0.6 and Bretschneider wave spectrum for Sea State 4.

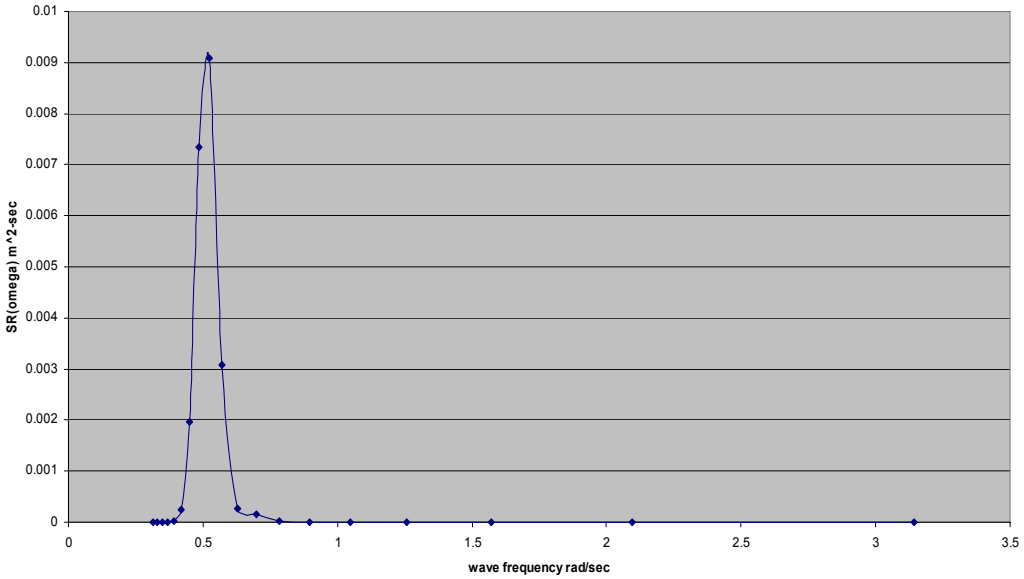

Figure 8. Ship response spectrum for generic trimaran at Sea State 4

The measure often used for the ship response to waves is the root mean square (RMS) of the time history of the response. [20] RMS is the integral of the response spectrum over increments of encounter frequency.

$$RMS = \int_0^\infty S_R(\omega_e)\, d\omega_e \tag{3.44}$$

The above integral is calculated numerically with a quadrature rule.

IV. SWAN 2 IMPLEMENTATION

A. NUMERICAL SOLUTION

SWAN-2 (Ship Wave Analysis) is a ship flow simulation in calm water and in waves. This computational fluid dynamics software was developed in Ocean Engineering Department at Massachusetts Institute of Technology. SWAN 2 solves three dimensional time-domain ship-wave interaction problem for steady and unsteady conditions by using Rankine Panel Method for a body with or without uniform speed. Basic outline of the Rankine Panel Method was described in the previous chapter. This chapter shows the basic theory and assumptions of the computer code. More details can be found in the theory and user manuals of SWAN2 2002 [12],[21]

1. Spatial Discretization

The ship boundary S_B and free surface S_F are divided into a large number of quadrilateral panels within defined boundaries. The velocity potential, φ and the wave elevation, ζ over the $j-th$ panel are approximated by bi-quadratic spline variation

$$\varphi(\vec{x},t) \cong \sum_j (\varphi)_j(t) B_j(\vec{x}) \tag{4.1}$$

$$\zeta(\vec{x},t) \cong \sum_j (\zeta)_j(t) B_j(\vec{x}) \tag{4.2}$$

where the basis function $B_j(x,y)$ is centered at the $j-th$ panel and the basis function provide continuity of (φ,ζ) between panels and their first tangential gradients [12]. Figure 9 shows half of the panel mesh due to the symmetry.

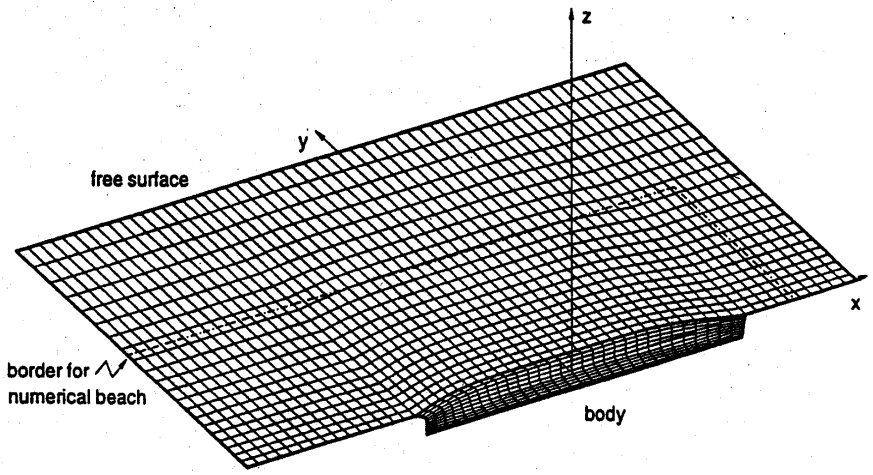

Figure 9. Discretization of ship hull and free surface (From Ref [21])

2. Temporal Discretization

By direct differentiation of expressions (4.1) and (4.2) over ship hull and free surface, tangential spatial derivatives may be evaluated. A time-marching scheme is selected for the approximation of velocity potential, φ and wave elevation, ζ in the time domain. The Euler marching is the scheme used by SWAN-2, which takes this form

$$\left(\frac{\partial \varphi}{\partial t}\right) \cong \frac{\varphi^{n+1} - \varphi^{n}}{\Delta t} \tag{4.3}$$

where the superscript n represents the time-step. The previous equation (4.3) is substituted in the free surface conditions, equations (3.10) and (3.11) and Green's identity (3.21) [12]

3. Radiation Conditions

The success of Rankine Panel Methods in simulating ship flows depends on the proper enforcement of the radiation condition. SWAN 2 introduces a wave-absorbing beach, comprises a layer of panels, which surrounds the free surface mesh. SWAN enforces following free surface conditions over the dissipative beach for the wave disturbance potential, φ

$$\left(\frac{\partial}{\partial t} - U\frac{\partial}{\partial x}\right)\zeta = \frac{\partial \varphi}{\partial z} - 2\nu\zeta + \frac{\nu^2}{g}\varphi \tag{4.4}$$

$$\left(\frac{\partial}{\partial t} - U\frac{\partial}{\partial x}\right)\varphi = -g\zeta \tag{4.5}$$

ν is the strength of the damping parameter and it is selected such that its value increases towards the outwards edge of the beach. Its value is zero for continuity reasons over inner edge of the beach.[12] These free surface conditions lead to dispersion relation at zero speed

$$\omega = i\nu \pm \sqrt{gk} \tag{4.6}$$

B. MESHING

SWAN-2 assembles panel sheets through the domain boundaries, namely the free surface, S_F and ship surface, S_B. Each panel sheet has a rectangular topology which is defined by a $M \times N$ mesh of points. SWAN-2 enforces the velocity potential to vary in a bi-quadratic manner on all types of sheets. There are 7 types of sheets to discretize the domain boundaries around a broad variety of vessels. [21]

1. Spline Sheets for Mesh Generation

Type-1 sheet is the free surface sheet. The free surface conditions are applied for the wave elevation and the velocity potential in combination with Green's identity. The condition of second zero derivatives for velocity potential and wave elevation are applied at the boundaries.

Sheet Type 2 is the free surface wake type sheet. This sheet meets the ship hull upstream of transom stern. SWAN-2 enforces the same boundary conditions like Sheet Type-1 but Kutta-Type conditions of continuity are enforced at the upstream.

Type 3 sheets are similar to Type-1 but the domain has oval shape opposed to rectangular shape. Sheet Type 4,5 is used to discretize the entire ship hull or the components of the ship hull. Type 6 sheet is a fluid-domain lifting wake sheet that meets horizontal or vertical thin struts at trailing edge. SWAN-2 enforces Kutta-Type conditions at this trailing edge.

Last sheet type, Sheet Type 7 corresponds to the dissipative beach. This free surface sheet is designed to absorb the wave disturbance energy diffracted and radiated by the ship hull. Figure 10 illustrates 3D plot of mesh generation for a trimaran hull form.

The mesh generation of trimaran is comprised of seven spline sheets of panels which are described above. Four spline sheets on the body and transom surface, three spline sheets on the free surface and wake are used. Only the half of the ship is modeled for symmetry reasons. Modeling the half of the ship saves calculation time, [12],[21].

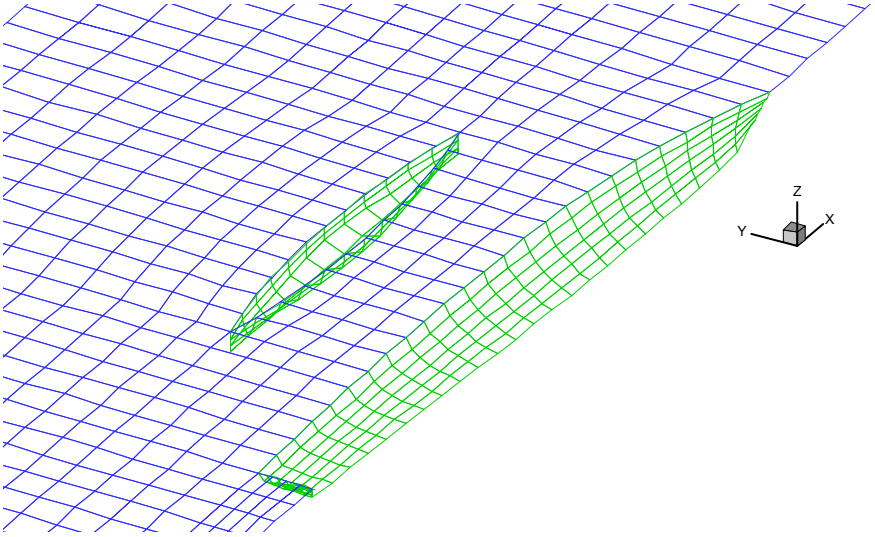

Figure 10. 3D Plot of Mesh Generation for Trimaran

2. Trimaran in SWAN-2

Basically, a trimaran hull form is comprised of main hull and two side hulls. Each hull is assumed to be symmetric in port-starboard direction for calculation purposes. The main hull may be either transom stern or cruiser stern and SWAN-2 performs the computation for infinite depth.

The length, beam and draft of the side hulls are described as percentage of length of the main hull. Also the location of the side hulls are input to SWAN-2 in both x and $y-axis$ in the form of X/Lpp and Y/Lpp. The code assumes the shape of the side hull to be mathematical form of modified Wigley hull. This mathematical hull form is defined as follows

$$\frac{y}{B}=\left[1-\left(\frac{x}{L}\right)^2\right]\left[1-\left(\frac{z}{T}\right)^2\right]\left[1+2\left(\frac{x}{L}\right)^2\right]+\left(\frac{z}{T}\right)\left[1-\left(\frac{x}{L}\right)^2\right]^4\left[1-\left(\frac{z}{T}\right)^8\right]$$

where the offsets of side hulls are evaluated by using this formula. L, B, and T are length, beam, and draft of the side hull. [21]

V. RESULTS

A. DISCUSSION

This chapter discusses response amplitude operators (RAOs) and root mean square (RMS) values of heave and pitch motions for a generic trimaran. Fine hull of the DDG-51 offsets were utilized to evaluate main hull of the generic trimaran. Basically, 466 ft length main hull was chopped off to 400 ft and half-breadths were decreased to half. Original 8:1 length to beam ratio was increased to 13:1 in order to enhance slenderness of the main hull. Basic dimensions and displacement of the trimaran;

L_{OA}=	123.20 m. (404.2 ft)	L_M / B_M =	13.0
L_{WL} =	121.92 m. (400 ft)	B_M =	9.403 m. (30.85 ft)
B=	27.315 m. (89.6 ft)	L_{side} =	38.10 m. (125 ft)
T=	3.6576 m. (12 ft)	B_{side} =	2.931 m. (9.616 ft)
Δ=	2506.54 metric ton (2466.96 LT)	L_{side} / B_{side} =	13.0
$(C_M)_{main}$ =	0.836	$(C_M)_{side}$ =	0.683
$(C_B)_{main}$ =	0.563	$(C_B)_{side}$ =	0.537
$(C_{WP})_{main}$ =	0.827	$(C_{WP})_{side}$ =	0.797

Table 2. Basic Dimensions of the Generic Trimaran

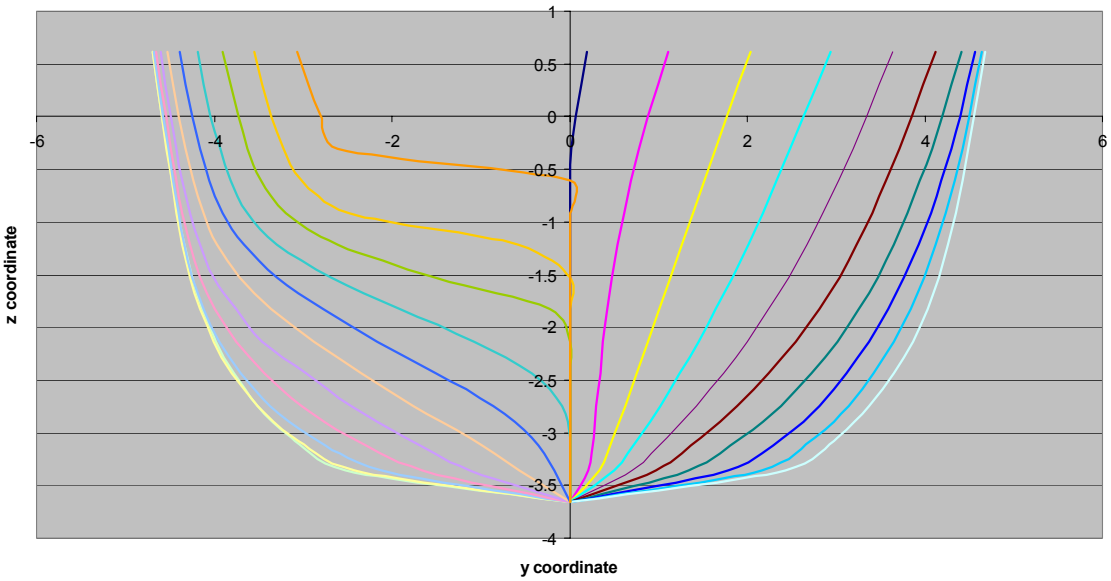

Figure 11. Body Plan of the Main Hull

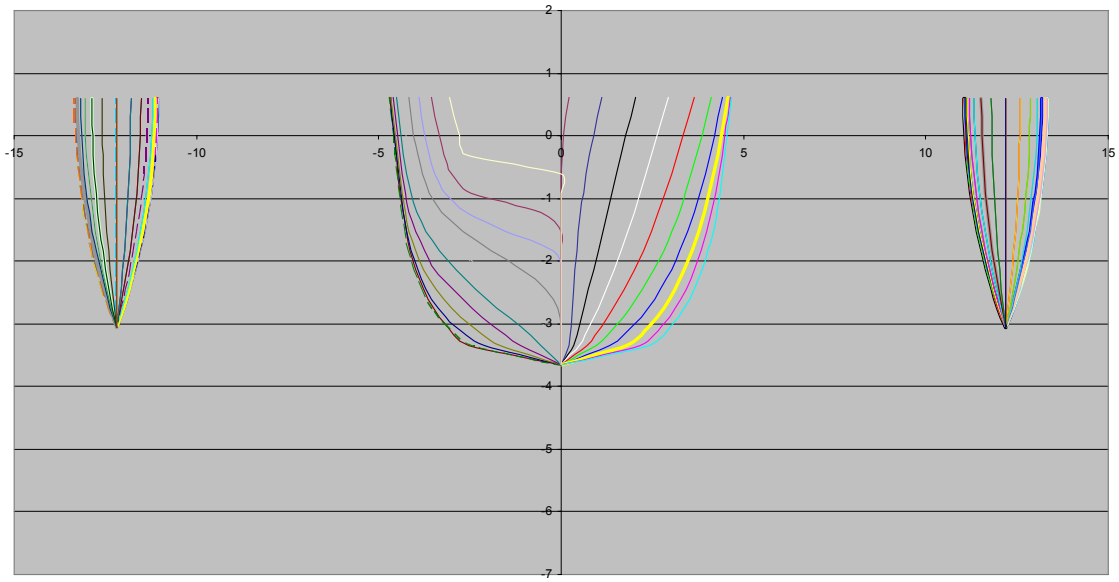

Figure 12. Body Plan of the Generic Trimaran

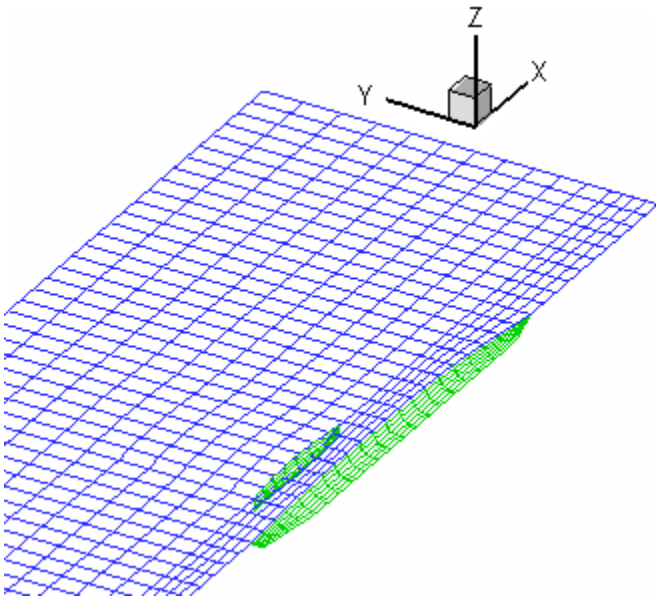

Figure 13. The Generic Trimaran Plotted by SWAN 2 , X/Lpp=0.3, Y/Lpp=0.1

The length of the side hulls was fixed to be 31.25% of the waterline length of the main hull. The length to maximum beam ratio was set to 13.0 to increase the slenderness of the side hulls as well as main hull. The maximum draft of the side hulls was adjusted to 2.5% of the main hull waterline length, slightly smaller than the draft of the main hull.

Three different positions in the y-direction and ten different positions in x-direction are analyzed in order to study the sensitivity of the dynamic response of the trimaran. We consider heave and pitch motions only for brevity. For comparison purposes, a ship that has favorable characteristics in these two modes of motion will also, generally speaking, exhibit favorable characteristics in all six degrees of freedom. A notable exception to this is of course roll, which depends heavily on the metacentric height. Since the latter is a function of the loading condition of the ship, it is not included in these parametric studies.

B. RESPONSE AMPLITUDE OPERATORS (RAO)

The heave and pitch response amplitude operators (RAO) are shown in the figures of this section. The RAO shows the amplitude of the response per unit wave amplitude in regular sinusoidal waves. It is essentially the frequency response function of the system, and is presented in terms of the nondimensional wave length of the incoming wave. Short wavelengths correspond to high frequency waves, while long wavelengths correspond to low frequencies.

Based on the presented plots, we can draw the following conclusions:

1. For relatively low forward speeds (low Froude numbers) and for head seas, it is possible to optimize the seakeeping performance of the ship by suitable longitudinal placement of the side hulls. Placement near amidships seems to be superior to aft/fore placements since it results in significantly lower RAOs.
2. This trend is not as clear for beam or quartering seas. Certain wavelengths result in higher response while other wavelengths result in lower RAOs.
3. As the Froude number increases, the situation becomes more complicated and certain results are reversed. Here, it is possible to induce less motions for fore or aft placements of the side hulls. This depends on the direction and wavelength of the incoming wave.
4. The final plots of this section present sample sensitivity results in terms of side hull placement for three different separation ratios. Closer placement of the side hulls exhibits better responses at short wavelengths. Again, no consistent trend can be established for both short and long wavelengths. Motion level depends on the frequency of the excitation.

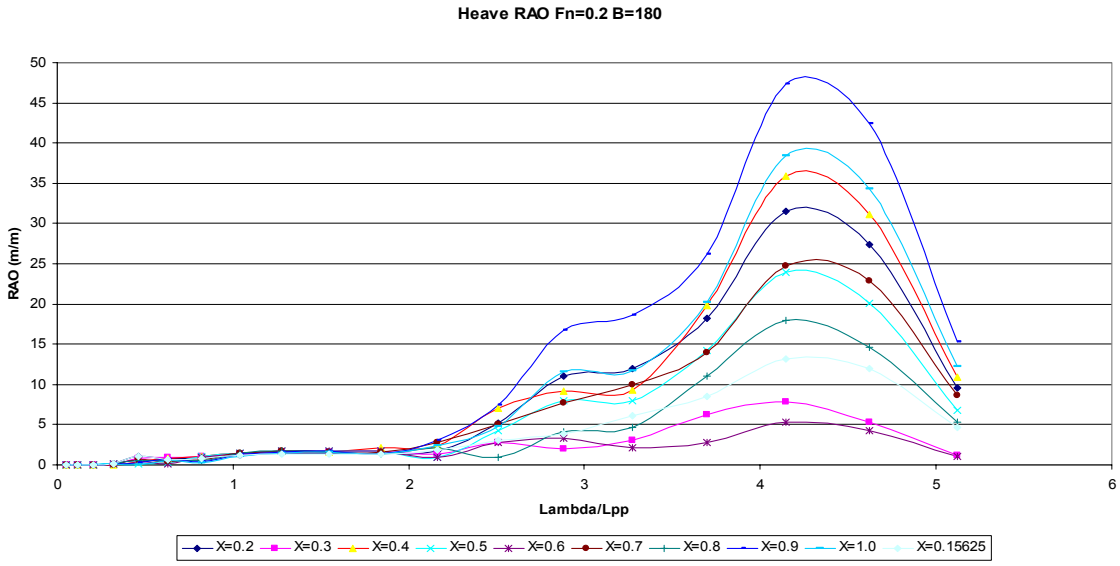

Figure 14. Fn=0.2 Heave Response Amplitude Operators for Head Seas

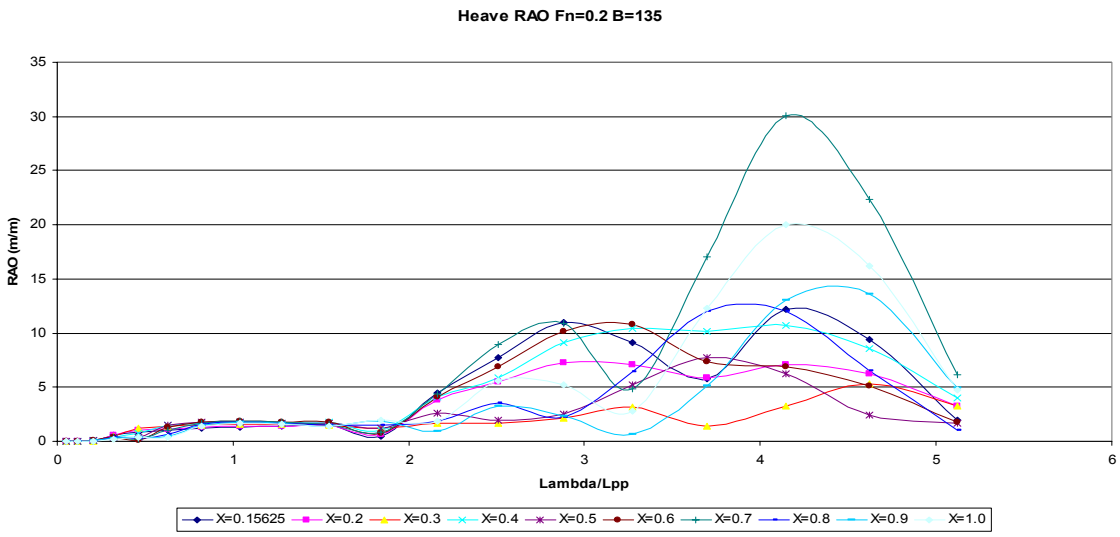

Figure 15. Fn=0.2 Heave Response Amplitude Operators for Bow Quartering Waves

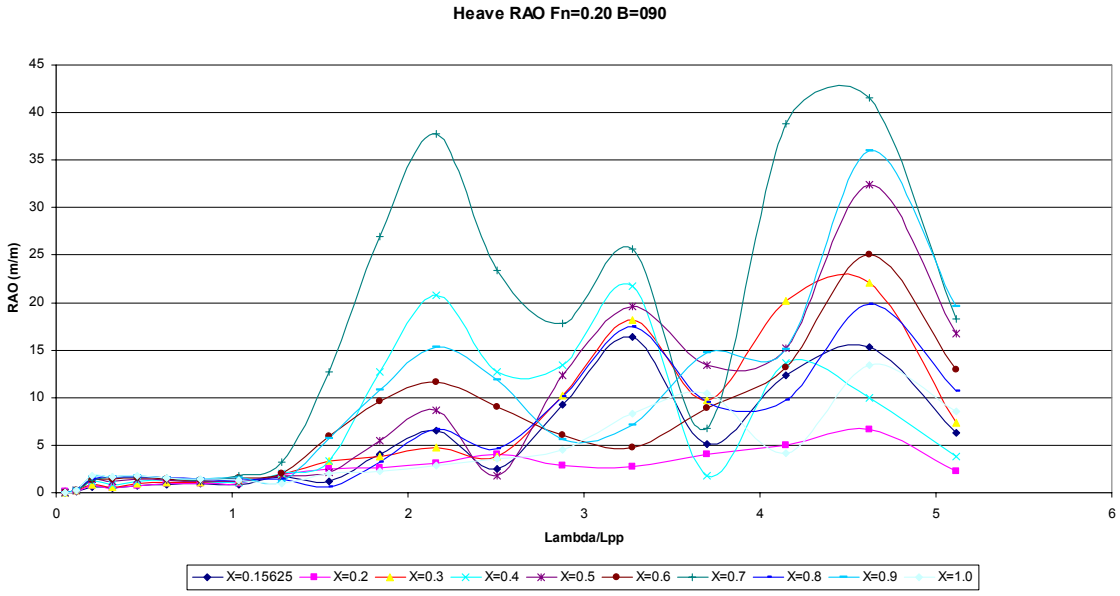

Figure 16. Fn=0.2 Heave Response Amplitude Operators for Beam Waves

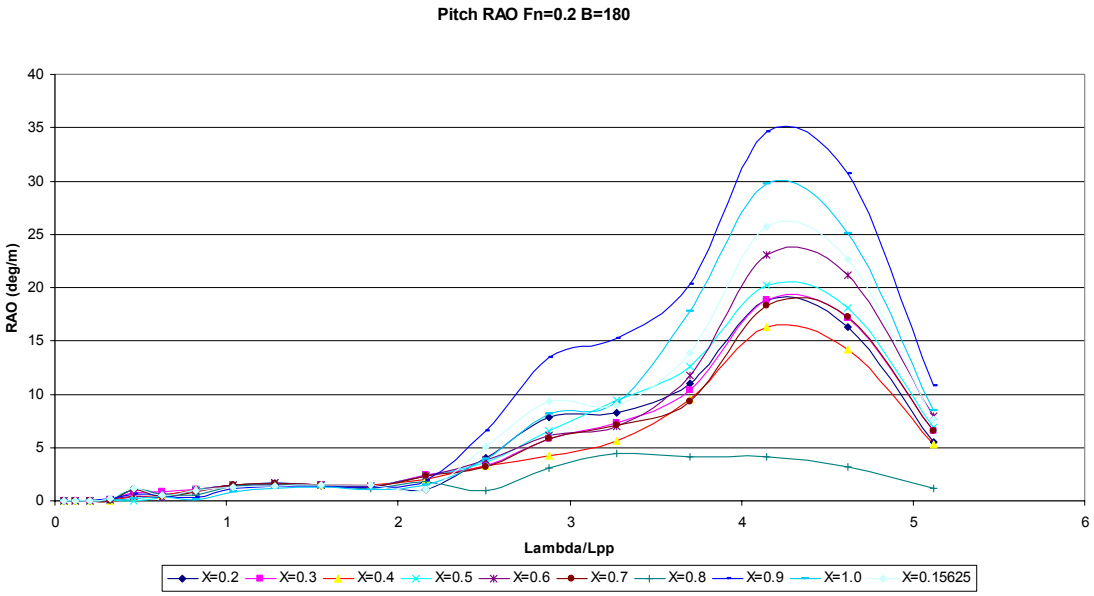

Figure 17. Fn=0.2 Pitch Response Amplitude Operators for Head Seas

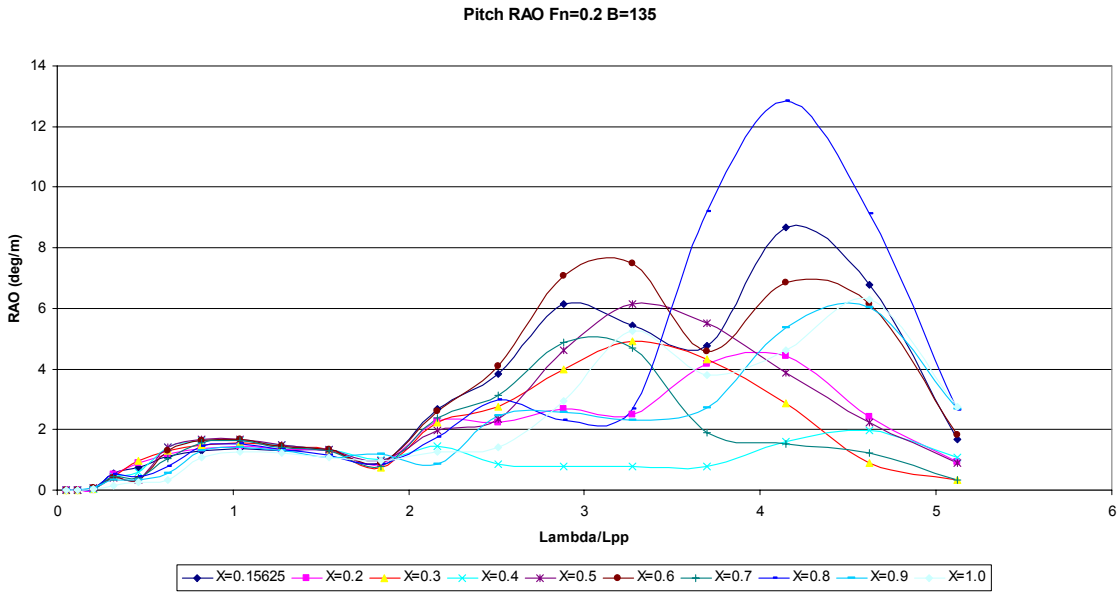

Figure 18. Fn=0.2 Pitch Response Amplitude Operators for Bow Quartering Waves

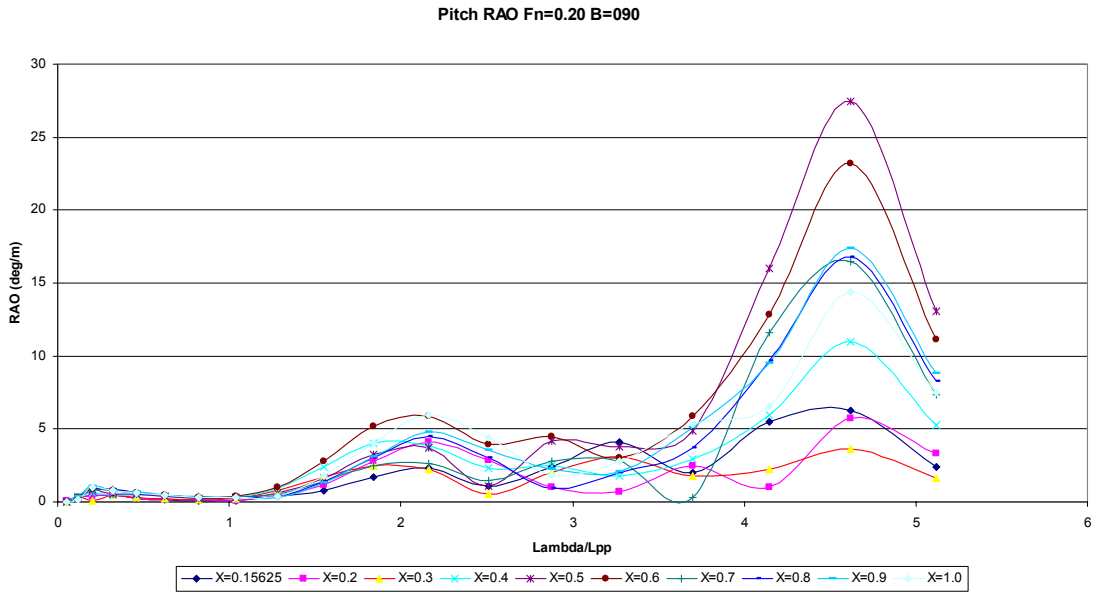

Figure 19. Fn=0.2 Pitch Response Amplitude Operators for Beam Waves

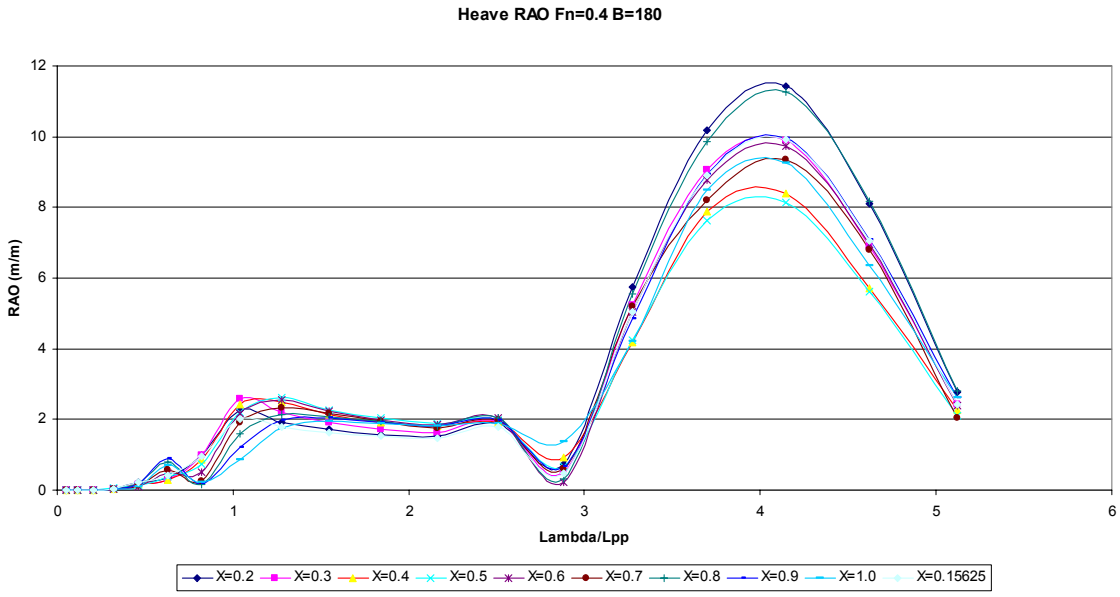

Figure 20. Fn=0.4 Heave Response Amplitude Operators for Head Seas

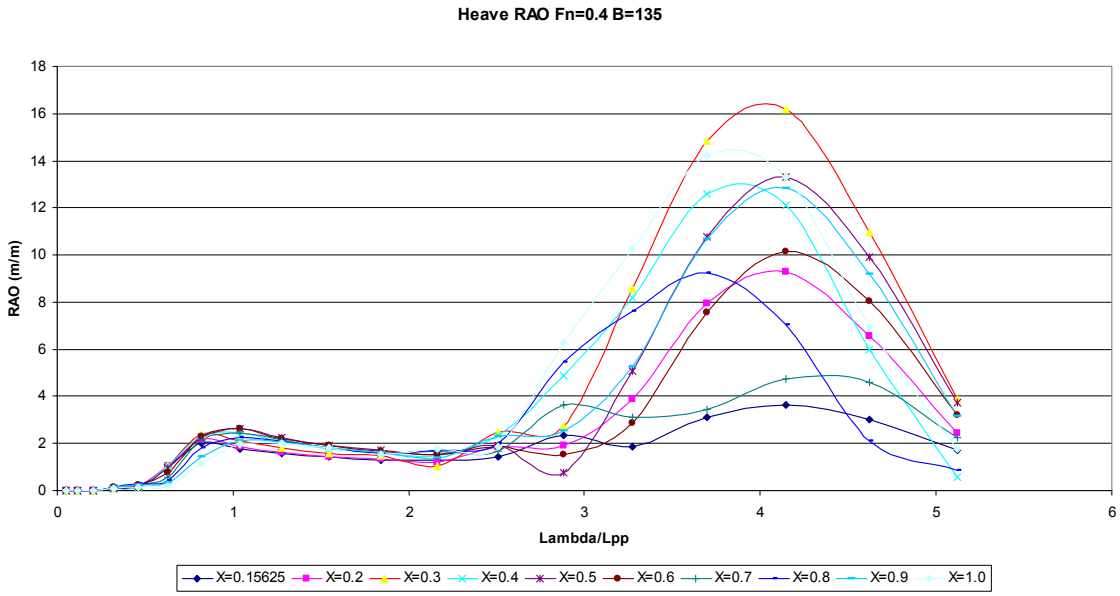

Figure 21. Fn=0.4 Heave Response Amplitude Operators for Bow Quartering Waves

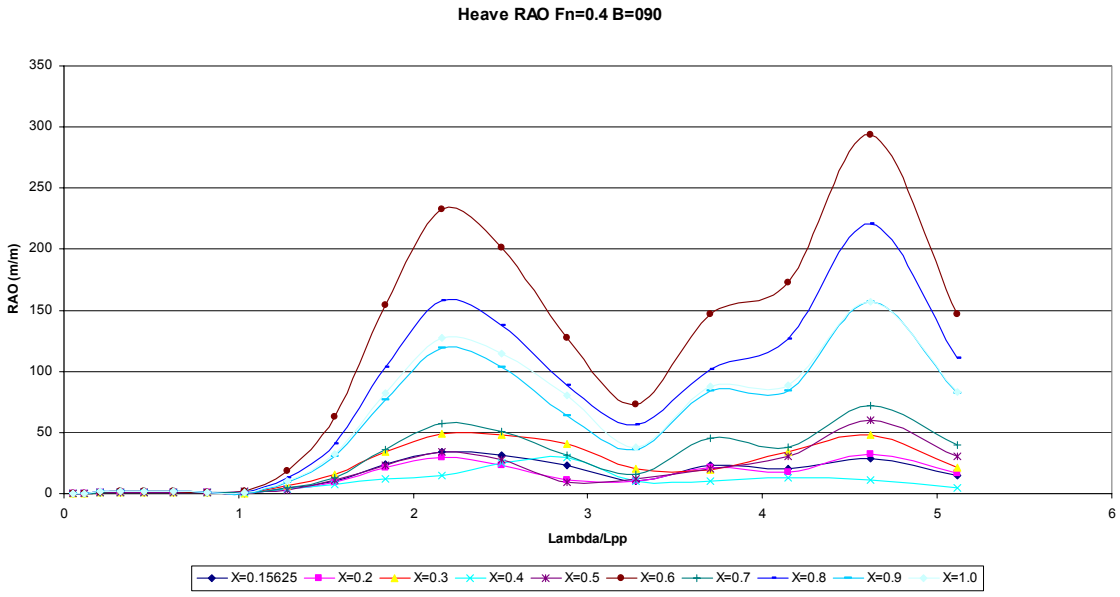

Figure 22. Fn=0.4 Heave Response Amplitude Operators for Beam Waves

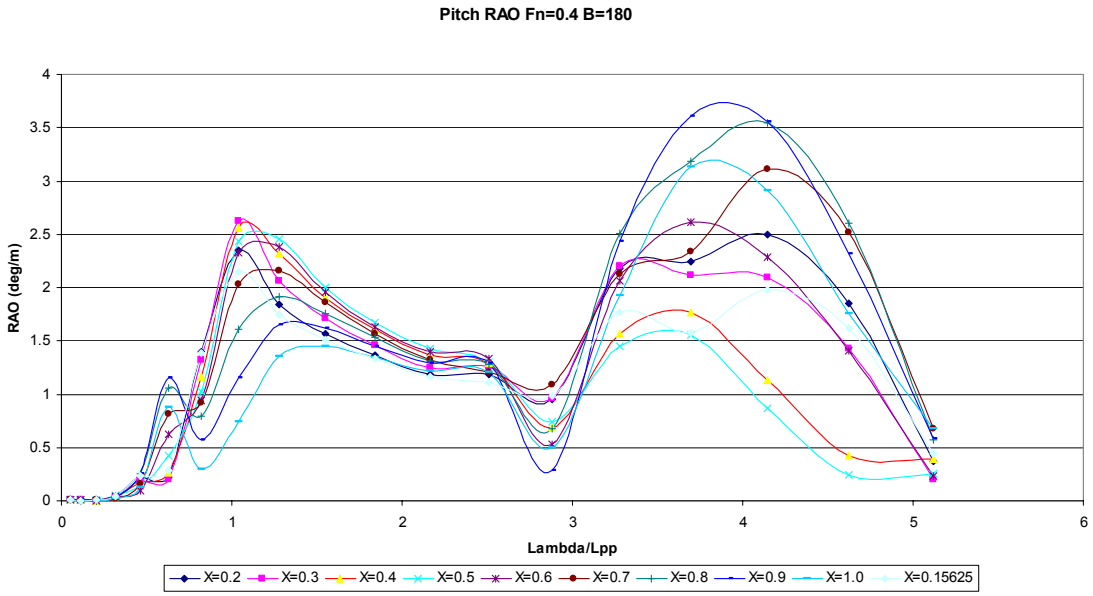

Figure 23. Fn=0.4 Pitch Response Amplitude Operators for Head Seas

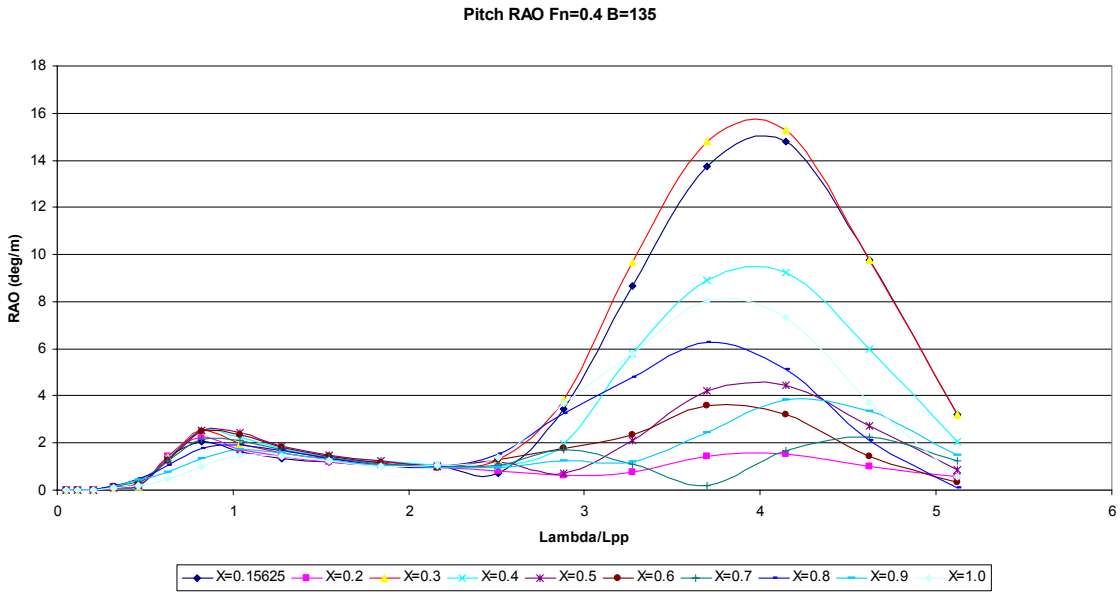

Figure 24. Fn=0.4 Pitch Response Amplitude Operators for Bow Quartering Waves

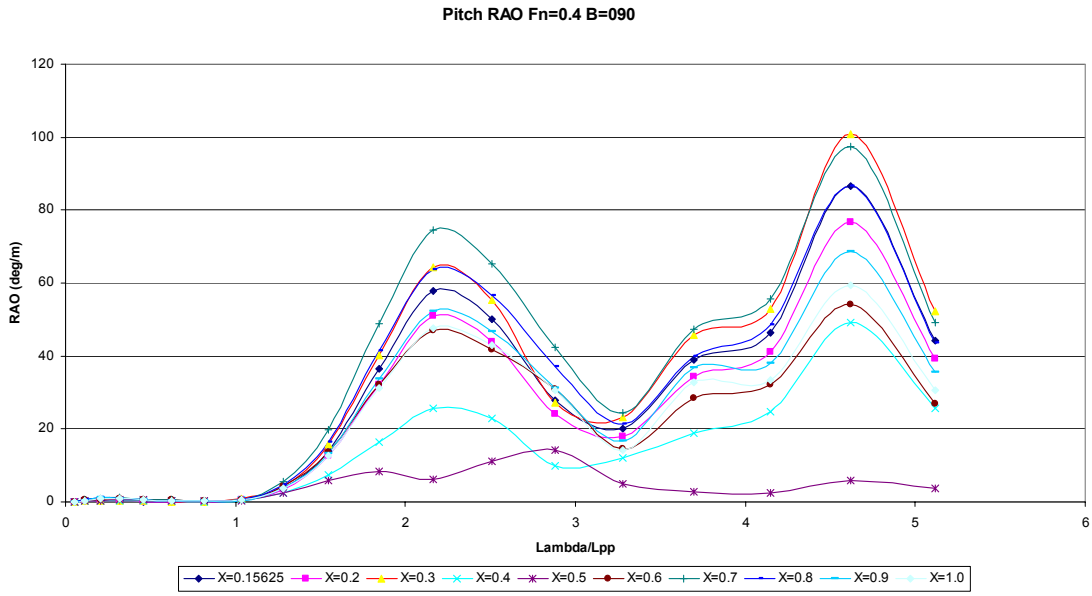

Figure 25. Fn=0.4 Pitch Response Amplitude Operators for Beam Waves

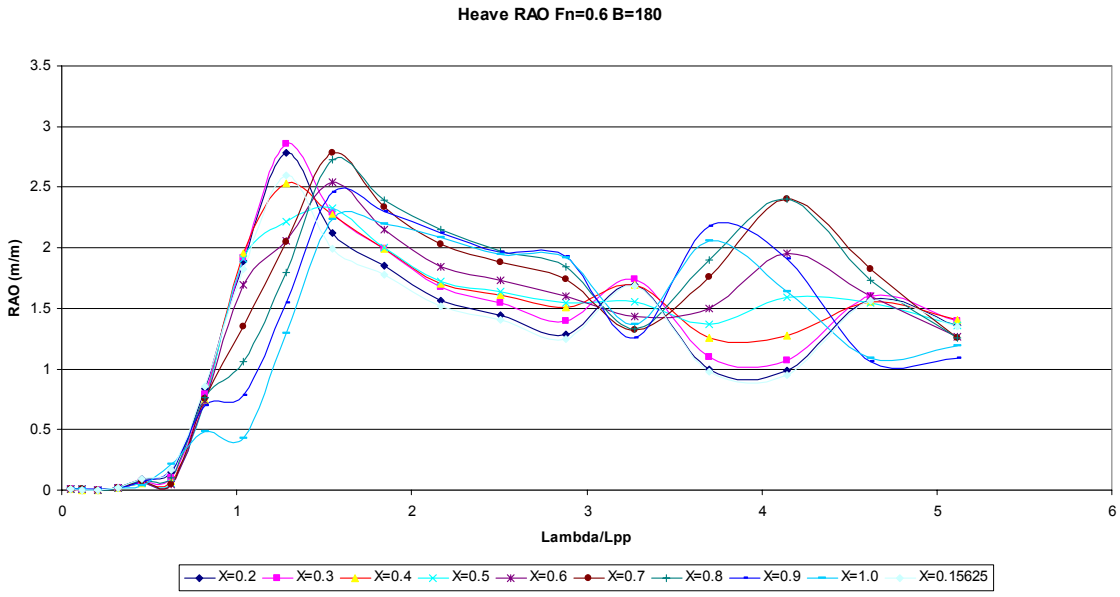

Figure 26. Fn=0.6 Heave Response Amplitude Operators for Head Seas

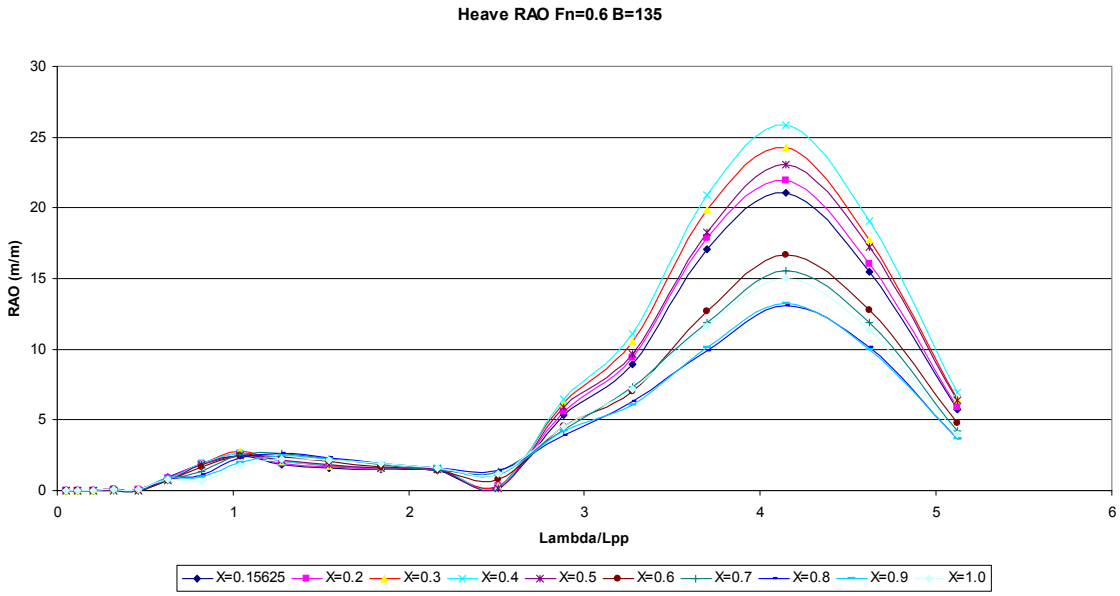

Figure 27. Fn=0.6 Heave Response Amplitude Operators for Bow Quartering Waves

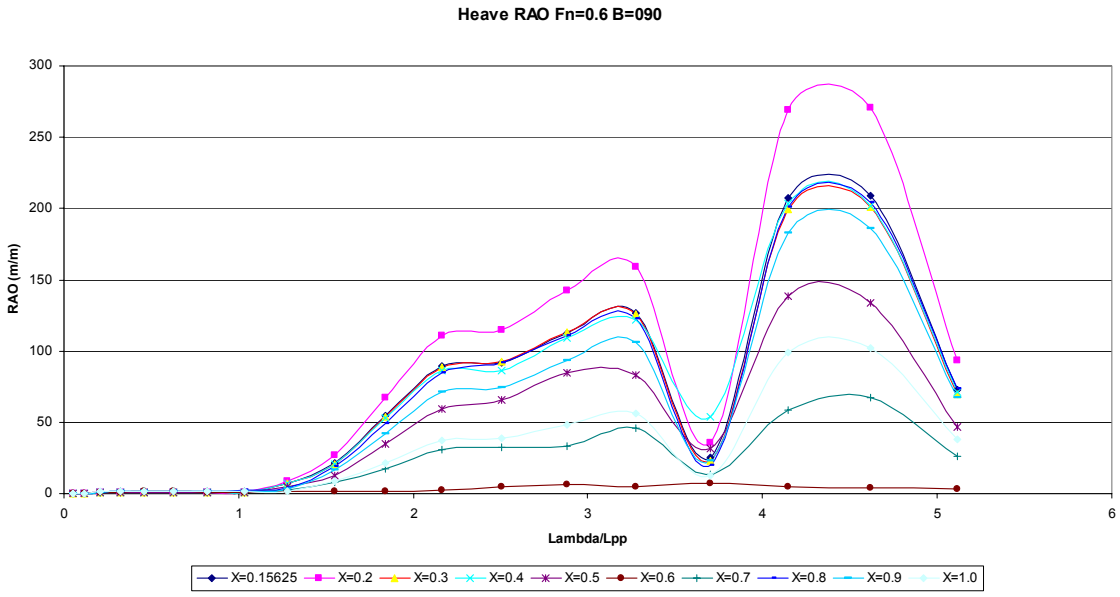

Figure 28. Fn=0.6 Heave Response Amplitude Operators for Beam Waves

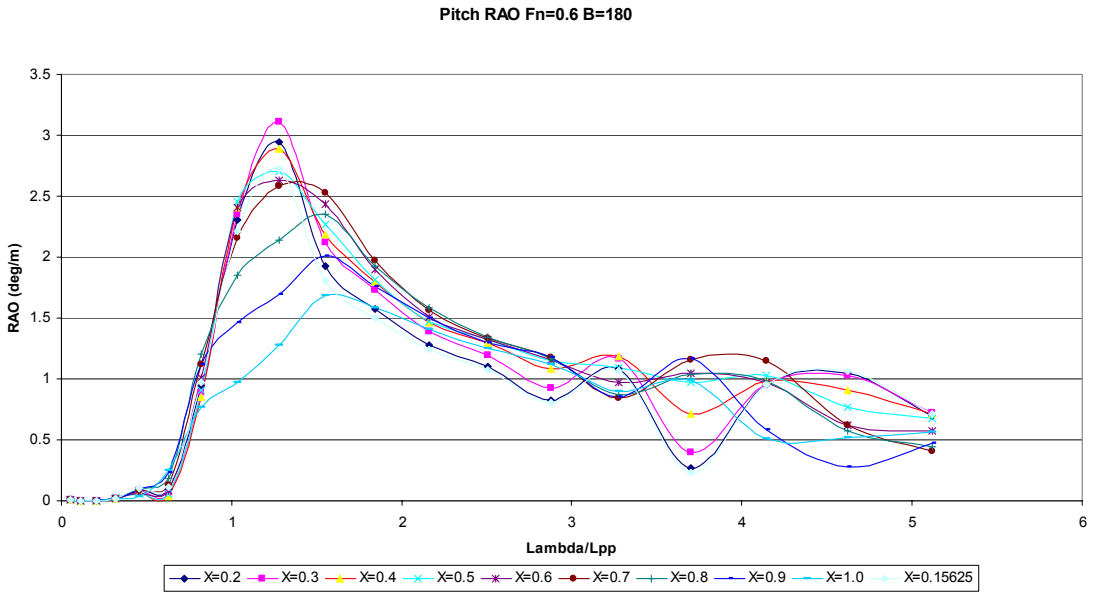

Figure 29. Fn=0.6 Pitch Response Amplitude Operators for Head Seas

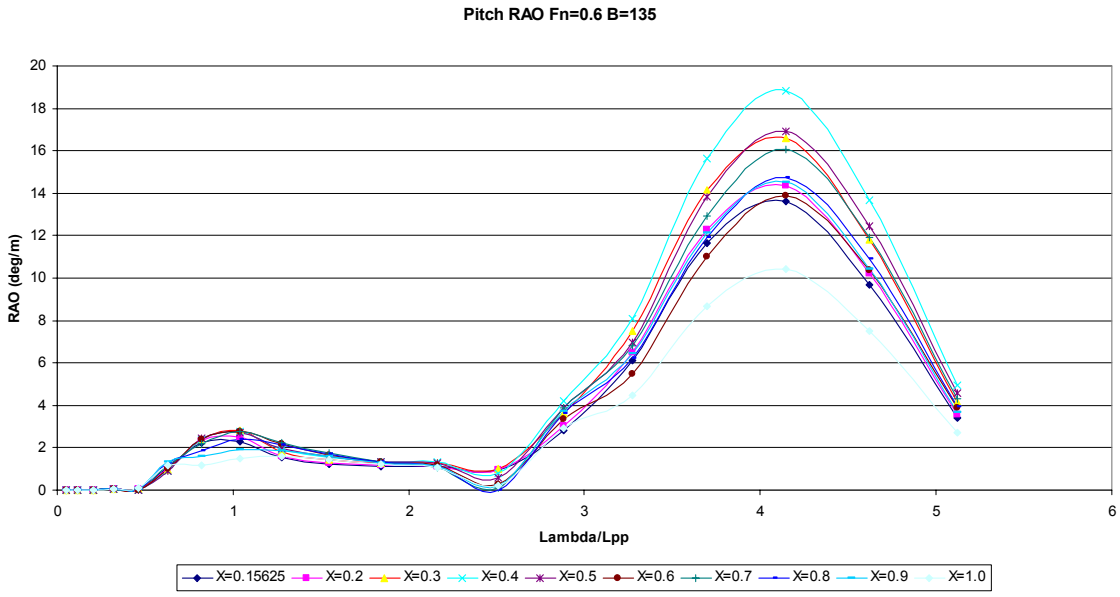

Figure 30. Fn=0.6 Pitch Response Amplitude Operators for Bow Quartering Waves

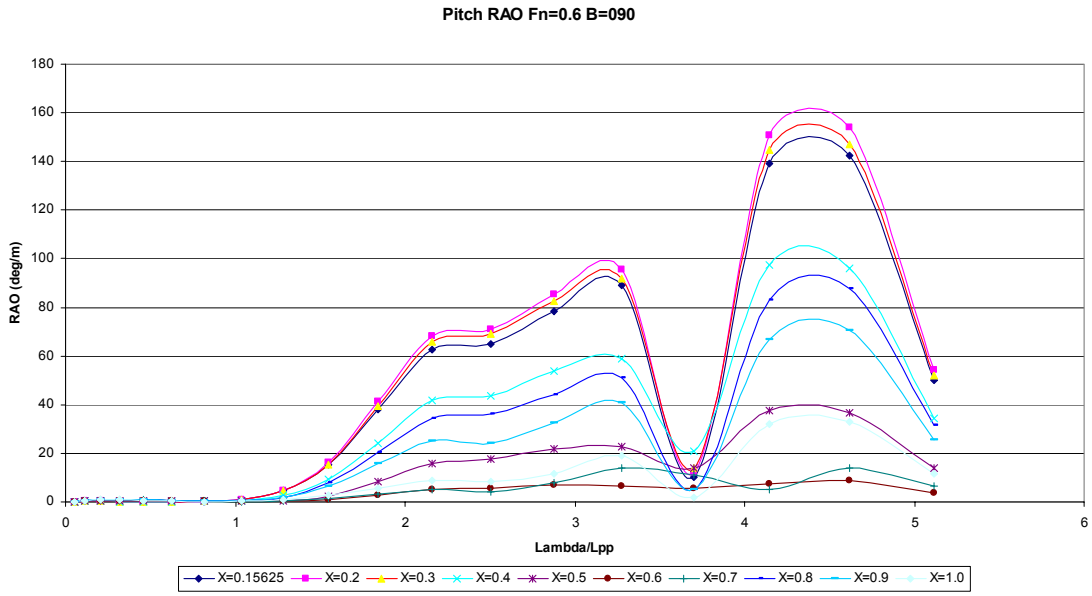

Figure 31. Fn=0.6 Pitch Response Amplitude Operators for Beam Waves

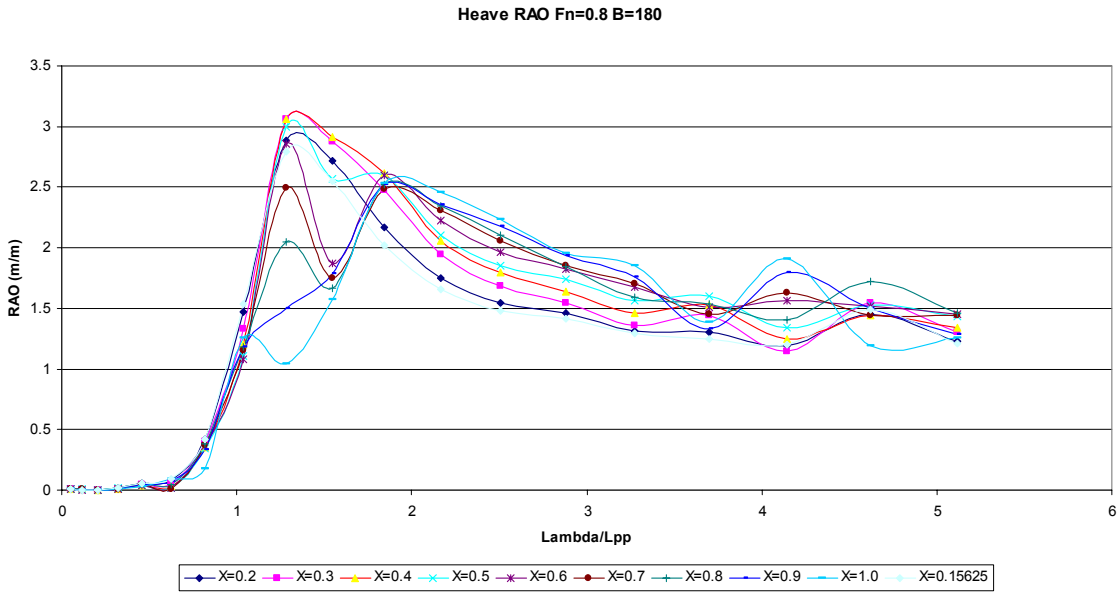

Figure 32. Fn=0.8 Heave Response Amplitude Operators for Head Seas

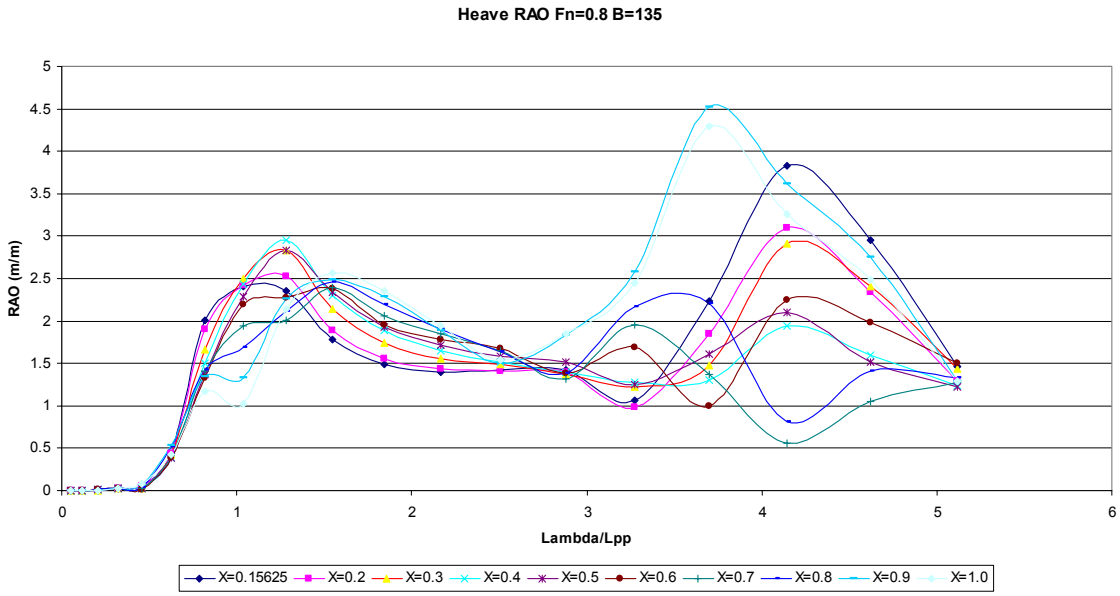

Figure 33. Fn=0.8 Heave Response Amplitude Operators for Bow Quartering Waves

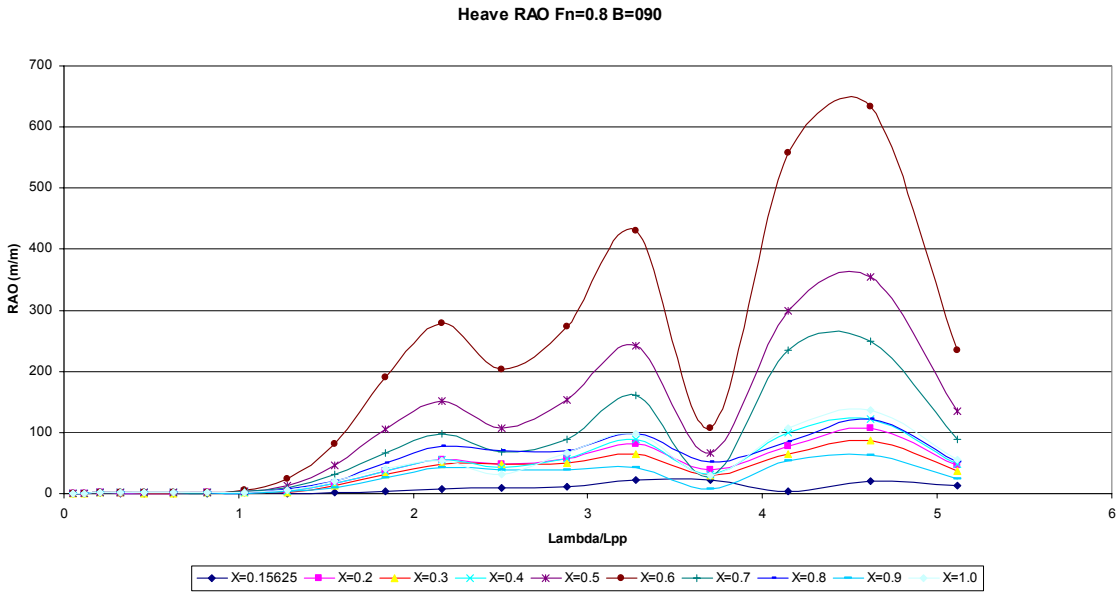

Figure 34. Fn=0.8 Heave Response Amplitude Operators for Beam Waves

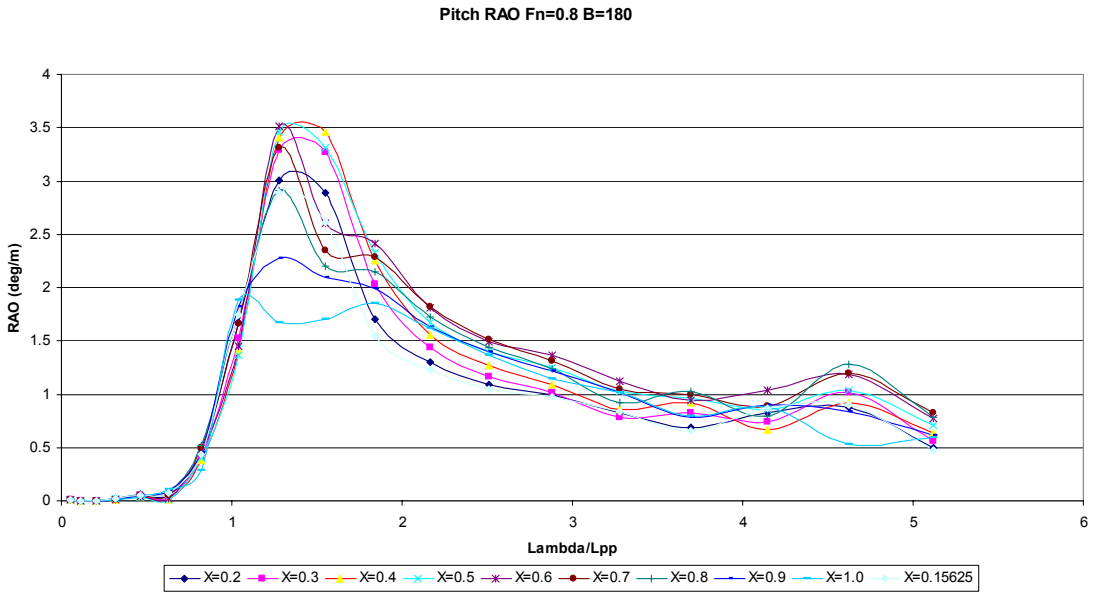

Figure 35. Fn=0.8 Pitch Response Amplitude Operators for Head Seas

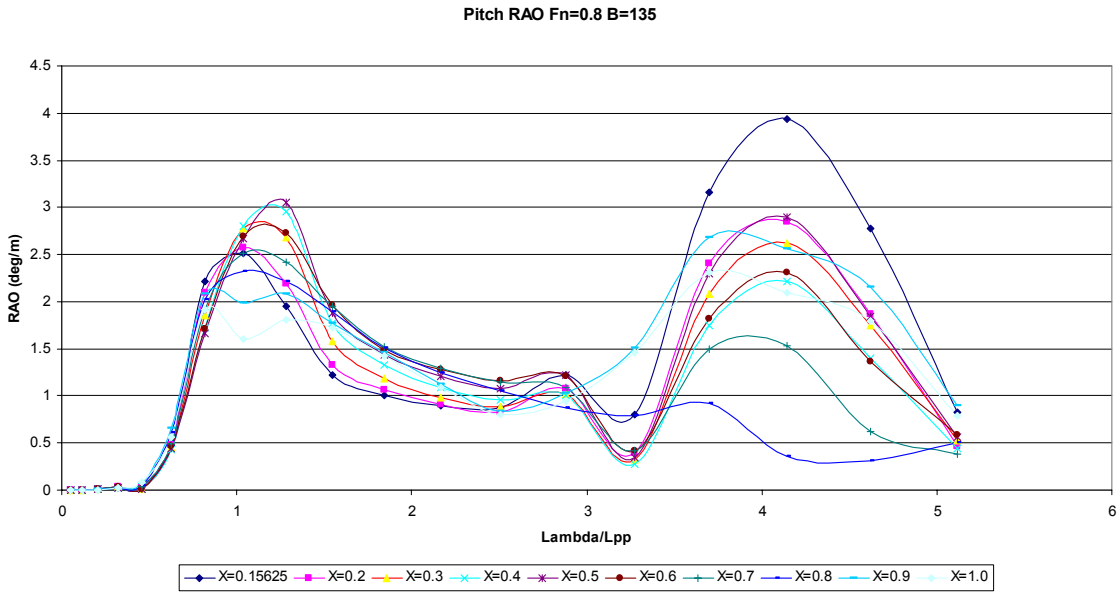

Figure 36. Fn=0.8 Pitch Response Amplitude Operators for Bow Quartering Waves

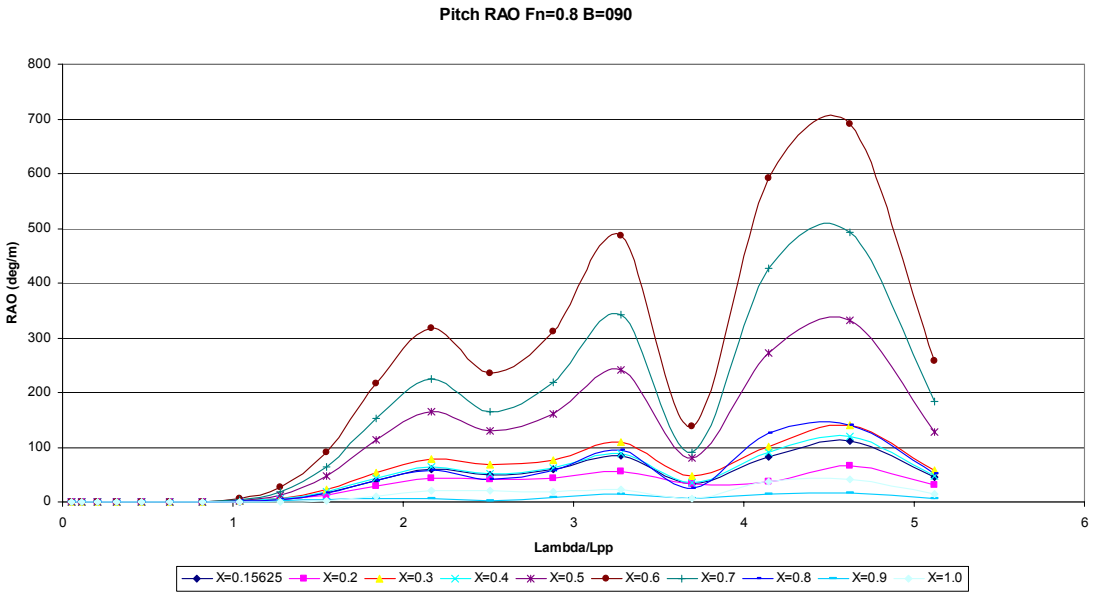

Figure 37. Fn=0.8 Pitch Response Amplitude Operators for Beam Waves

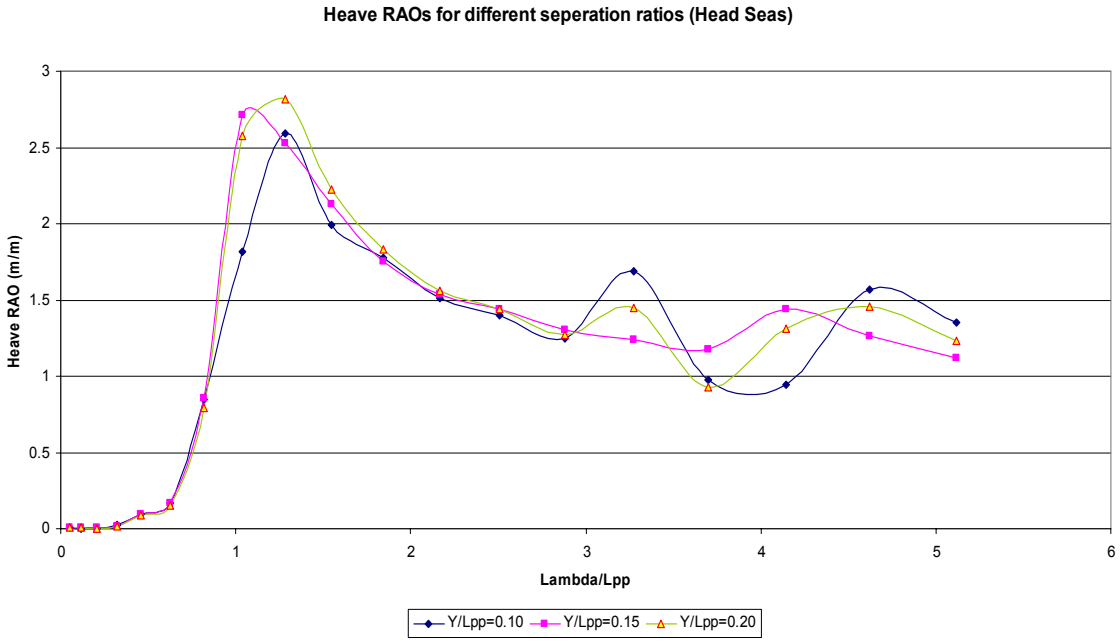

Figure 38. Heave RAOs at Different Separation Ratios for Head Seas

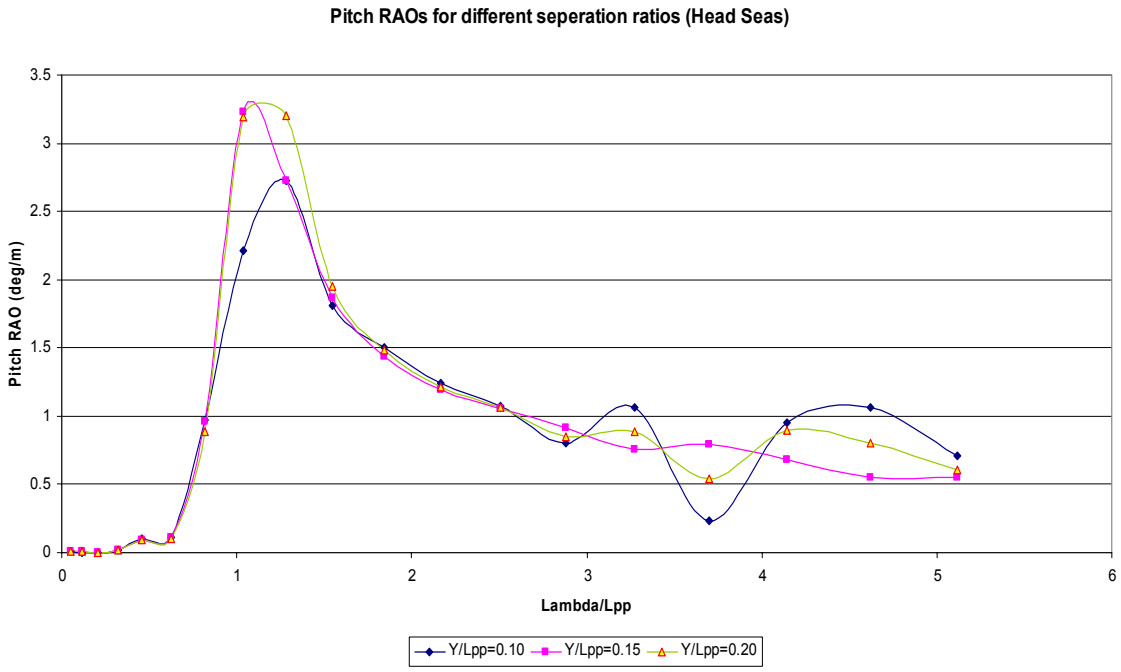

Figure 39. Pitch RAOs at Different Separation Ratios for Head Seas

C. ROOT MEAN SQUARE (RMS) VALUES

The following plots show the results in random seas. We utilized the two parameter Bretschneider spectrum for this analysis. All results are presented in terms of the heave or pitch root mean square (RMS). This is a significant design parameter since it is directly proportional to the maximum expected value of the response. Based on the presented results, we can draw the following conclusions:

1. With the exception of beam seas, which result in unrealistically high responses, we can see that in general, aft or fore placement of the side hulls results in lower RMS values.
2. Smaller values of the hull separation values result in better seakeeping behavior for head seas.
3. Higher forward speeds, Fn=0.6 and Fn=0.8, result lower RMS values for bow quartering waves and head seas.
4. Seakeeping response is highly dependent on forward speed and modal period.

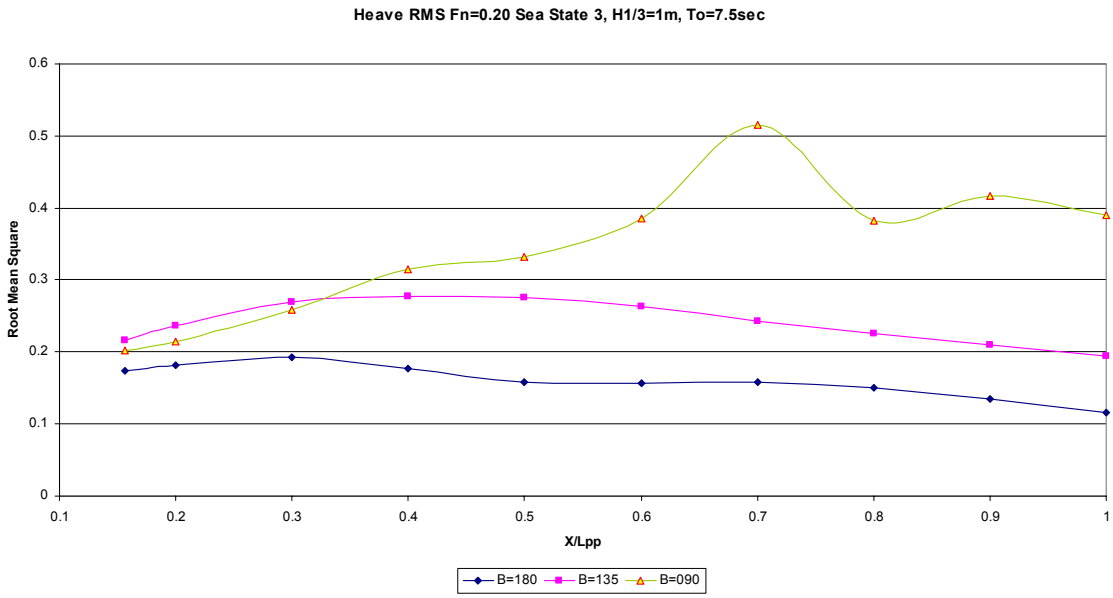

Figure 40. Fn=0.2 Heave RMS Values at Sea State 3 for Different Headings

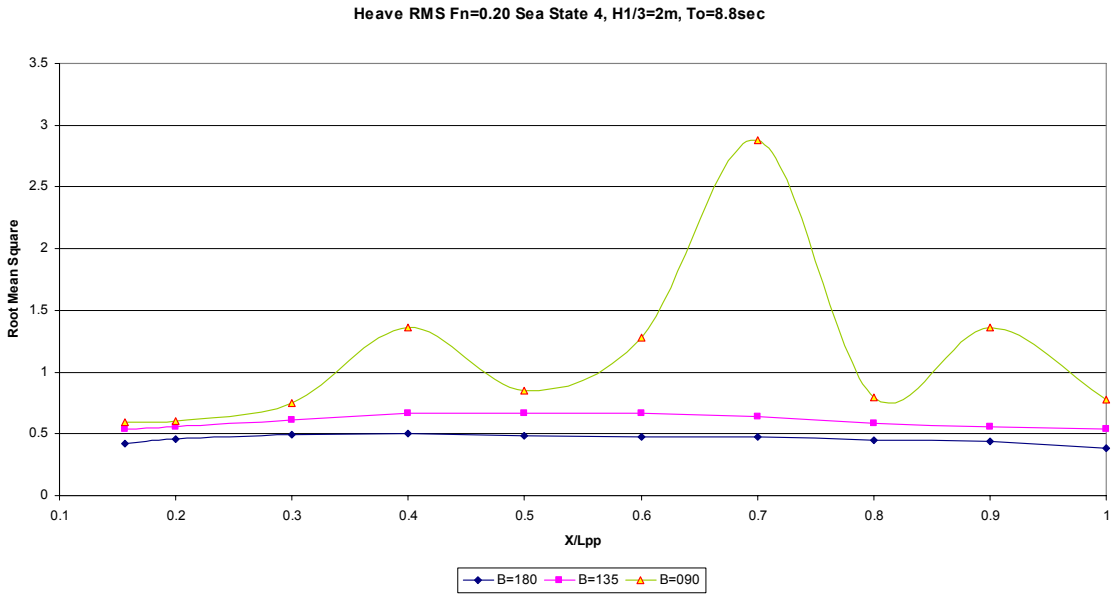

Figure 41. Fn=0.2 Heave RMS Values at Sea State 4 for Different Headings

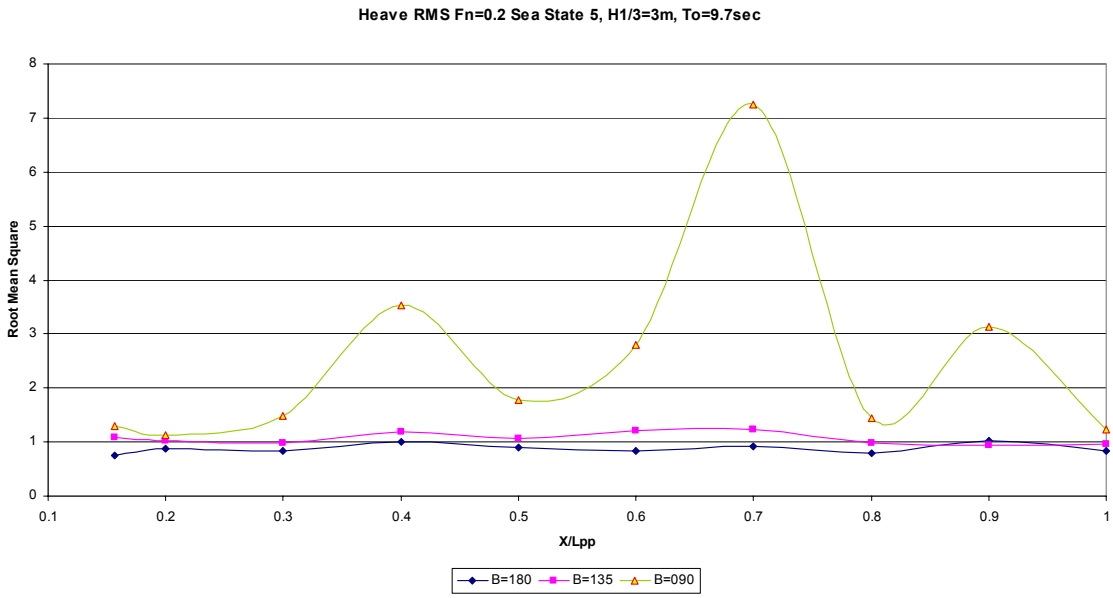

Figure 42. Fn=0.2 Heave RMS Values at Sea State 5 for Different Headings

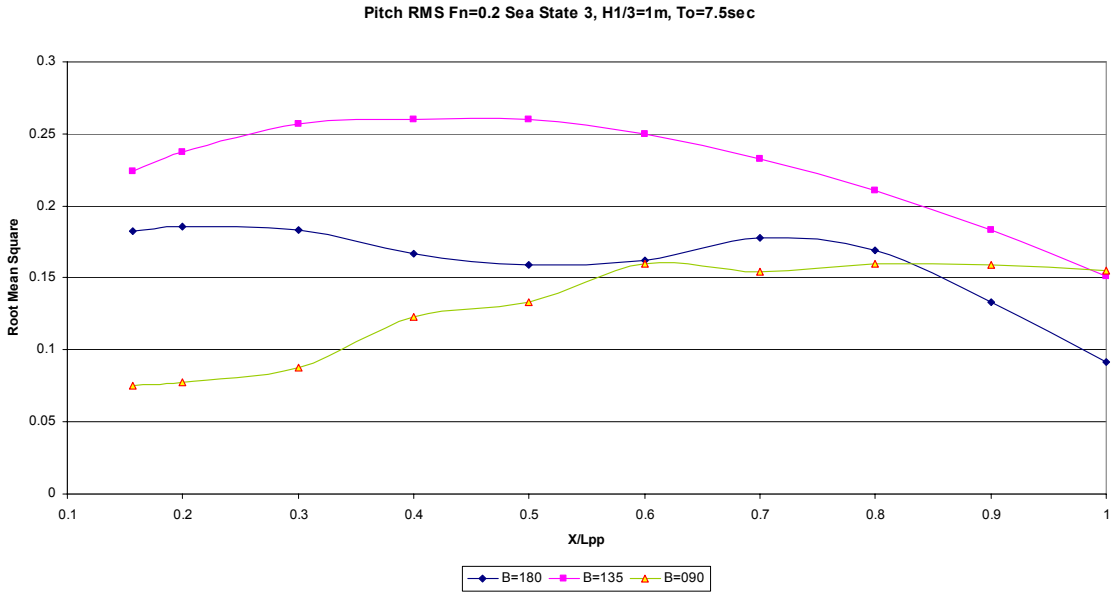

Figure 43. Fn=0.2 Pitch RMS Values at Sea State 3 for Different Headings

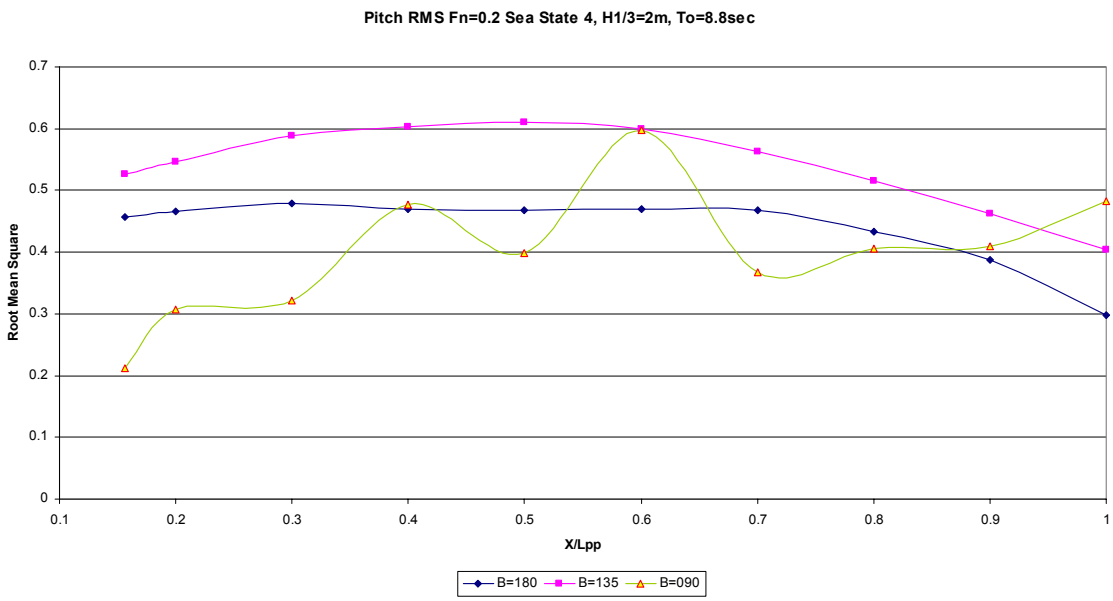

Figure 44. Fn=0.2 Pitch RMS Values at Sea State 4 for Different Headings

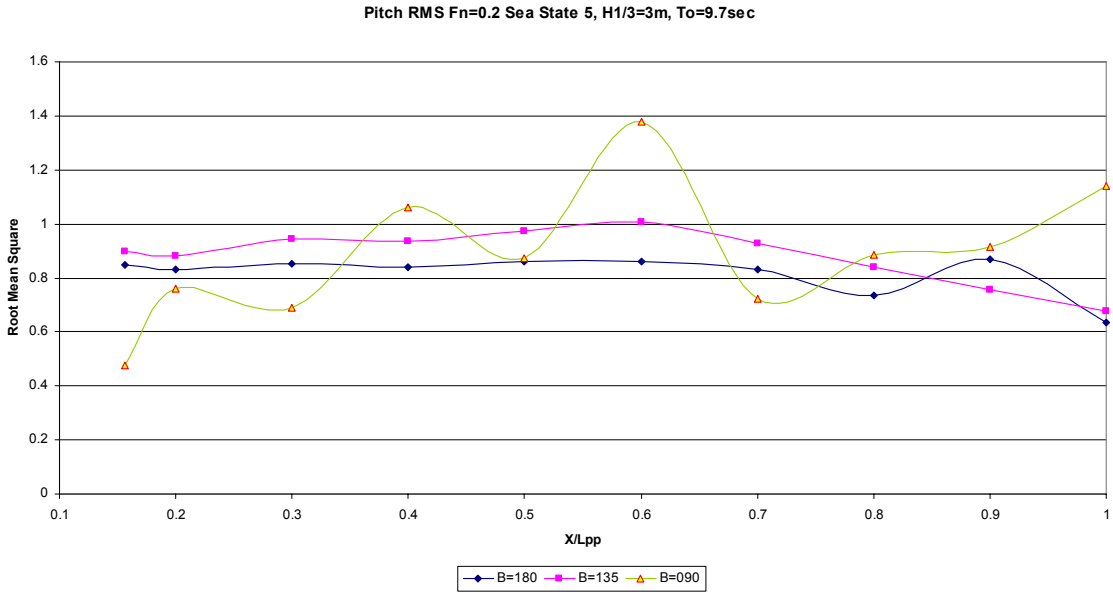

Figure 45. Fn=0.2 Pitch RMS Values at Sea State 5 for Different Headings

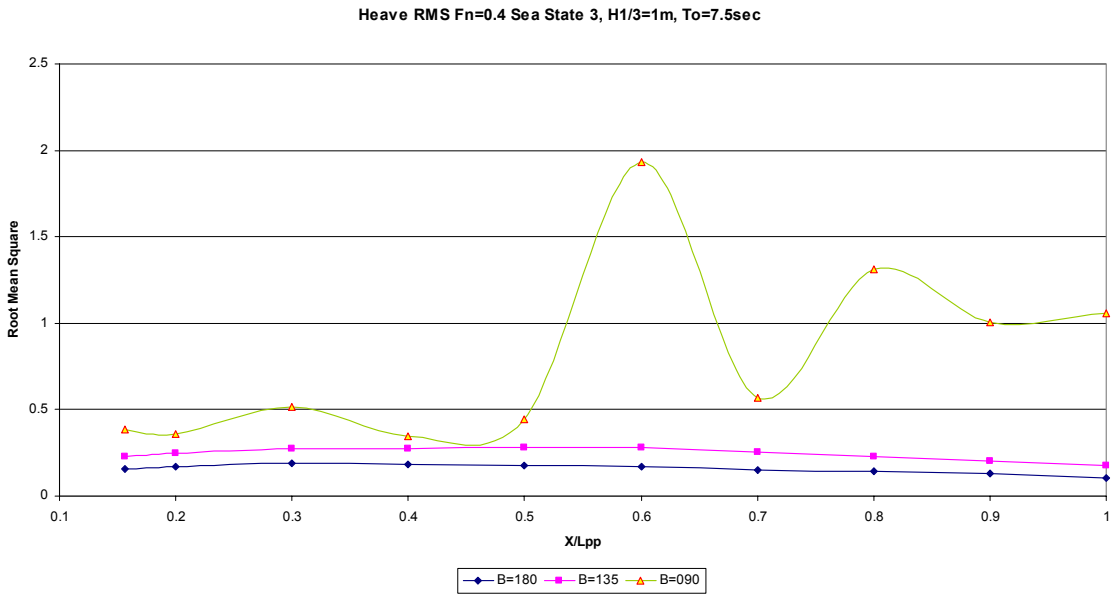

Figure 46. Fn=0.4 Heave RMS Values at Sea State 3 for Different Headings

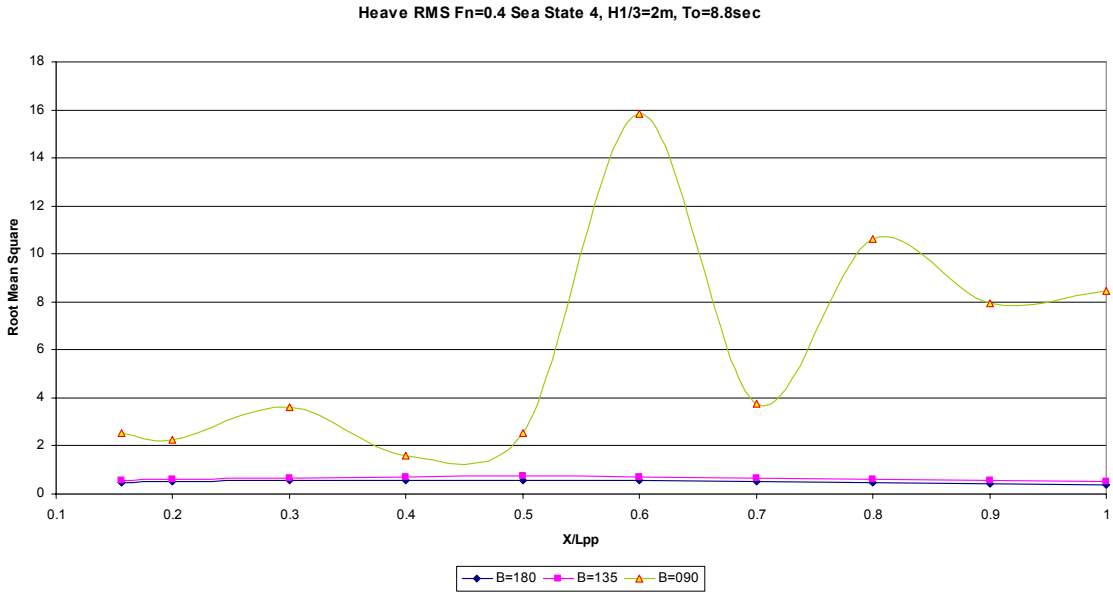

Figure 47. Fn=0.4 Heave RMS Values at Sea State 4 for Different Headings

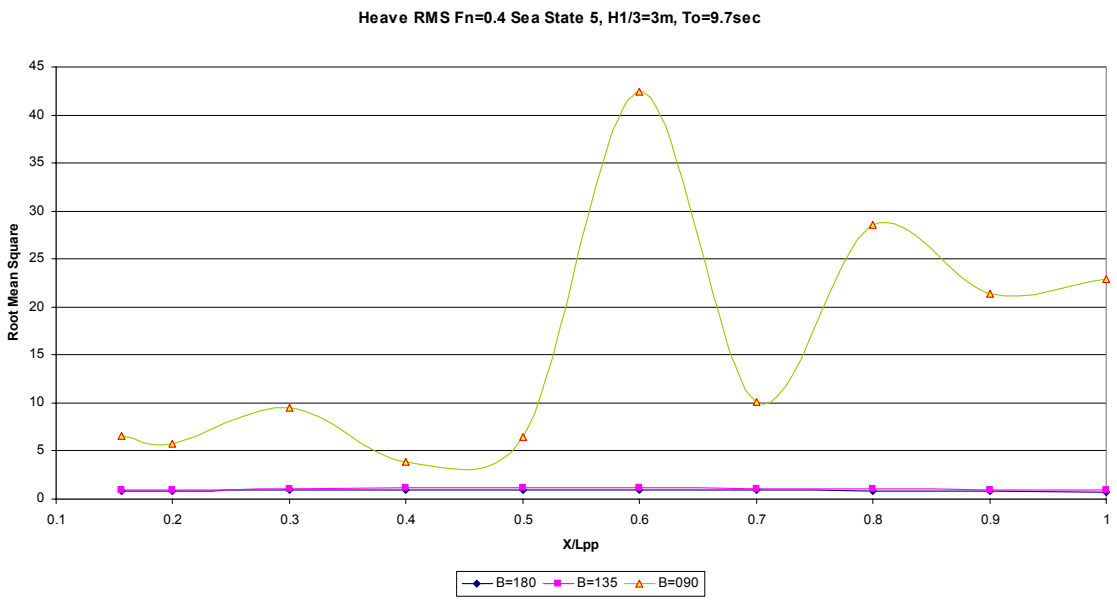

Figure 48. Fn=0.4 Heave RMS Values at Sea State 5 for Different Headings

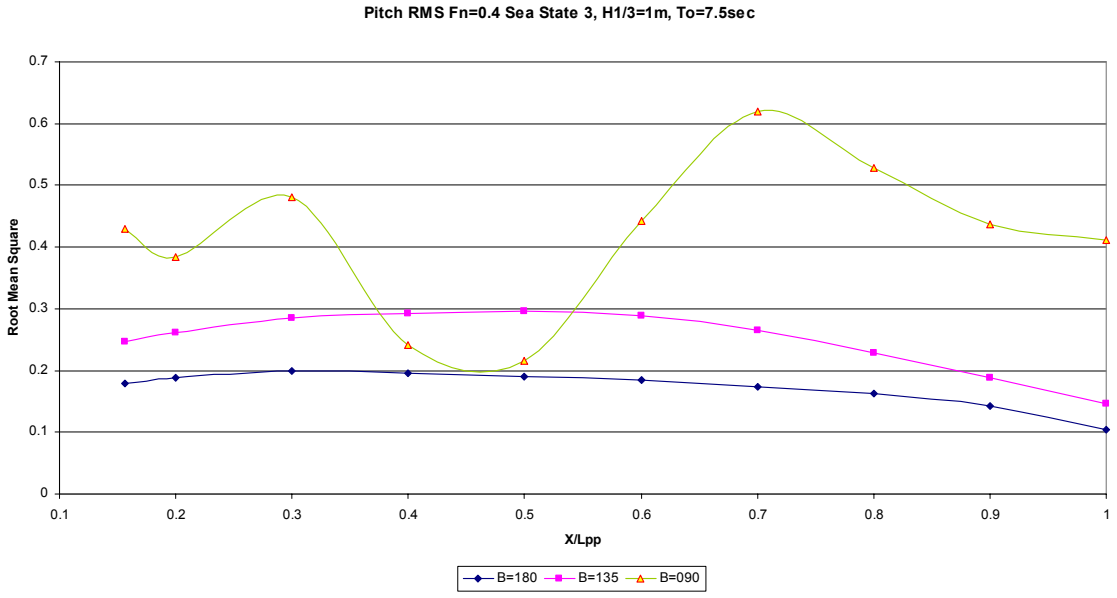

Figure 49. Fn=0.4 Pitch RMS Values at Sea State 3 for Different Headings

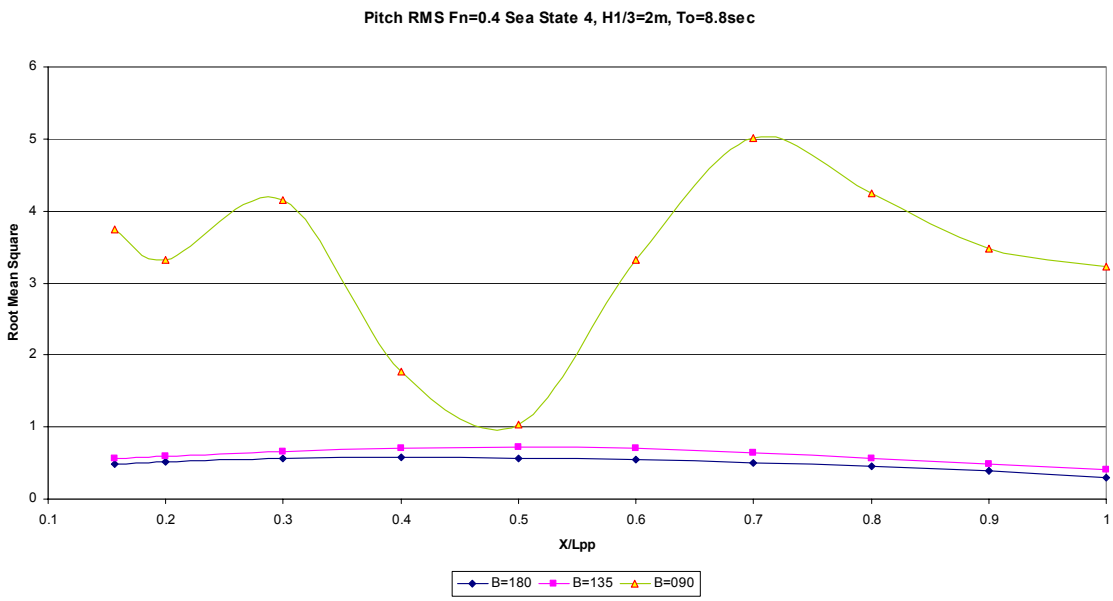

Figure 50. Fn=0.4 Pitch RMS Values at Sea State 4 for Different Headings

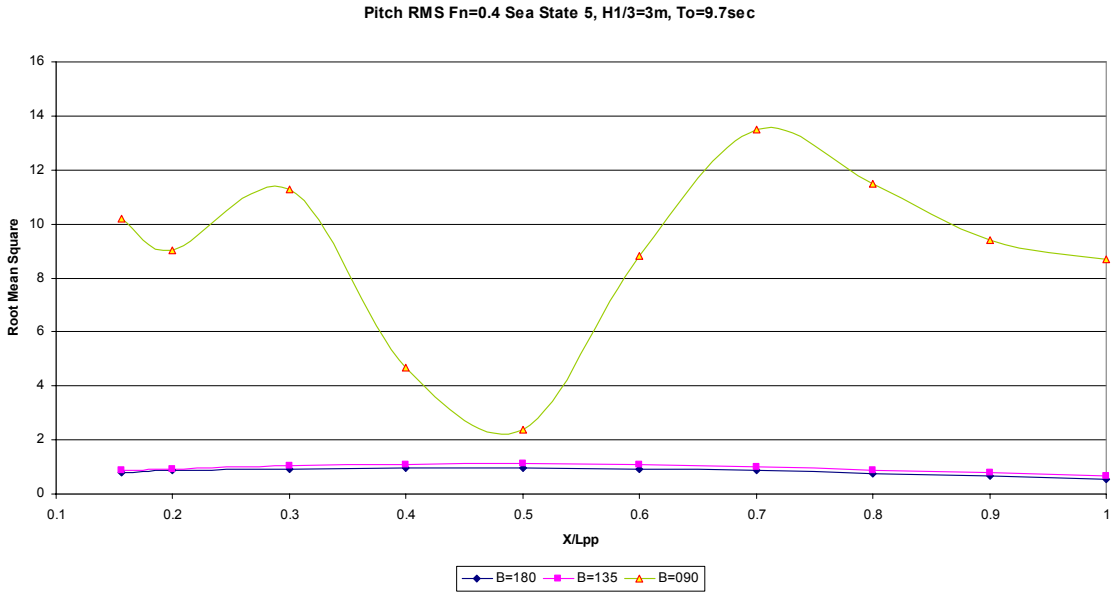

Figure 51. Fn=0.4 Pitch RMS Values at Sea State 5 for Different Headings

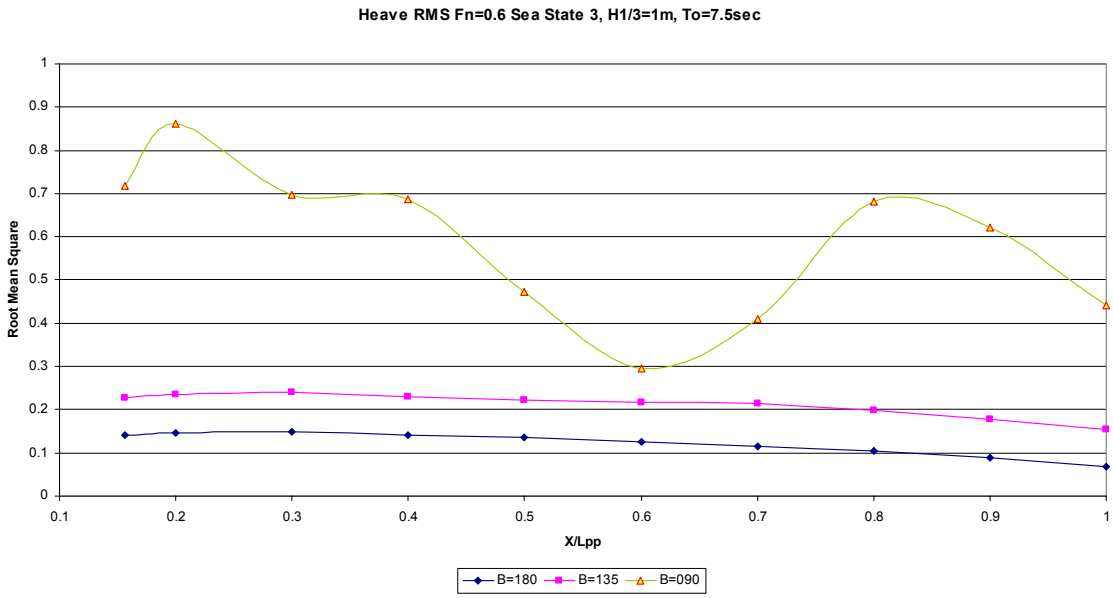

Figure 52. Fn=0.6 Heave RMS Values at Sea State 3 for Different Headings

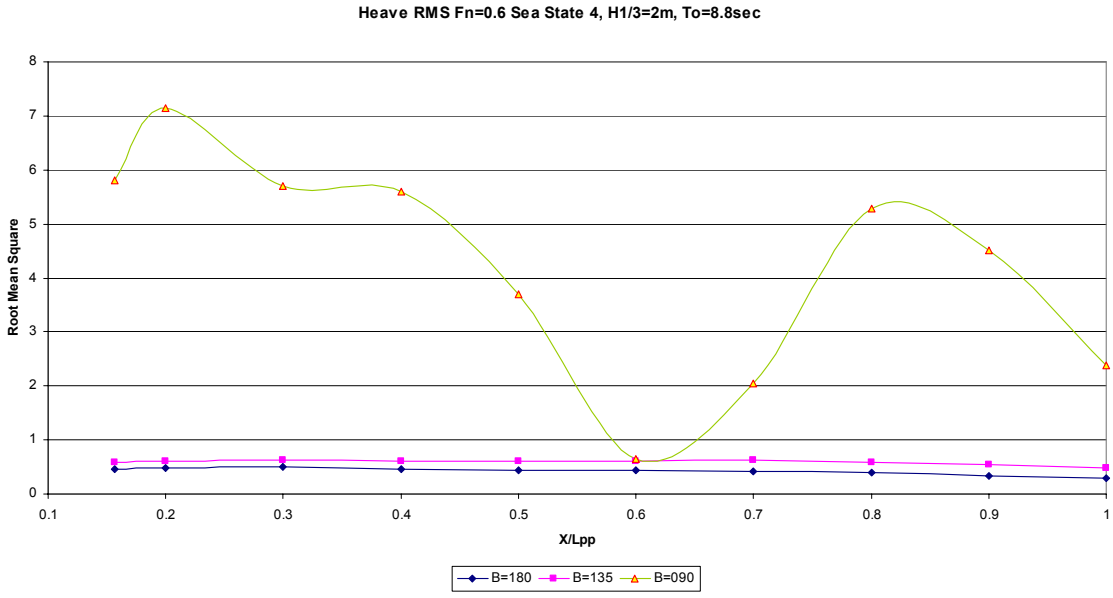

Figure 53. Fn=0.6 Heave RMS Values at Sea State 4 for Different Headings

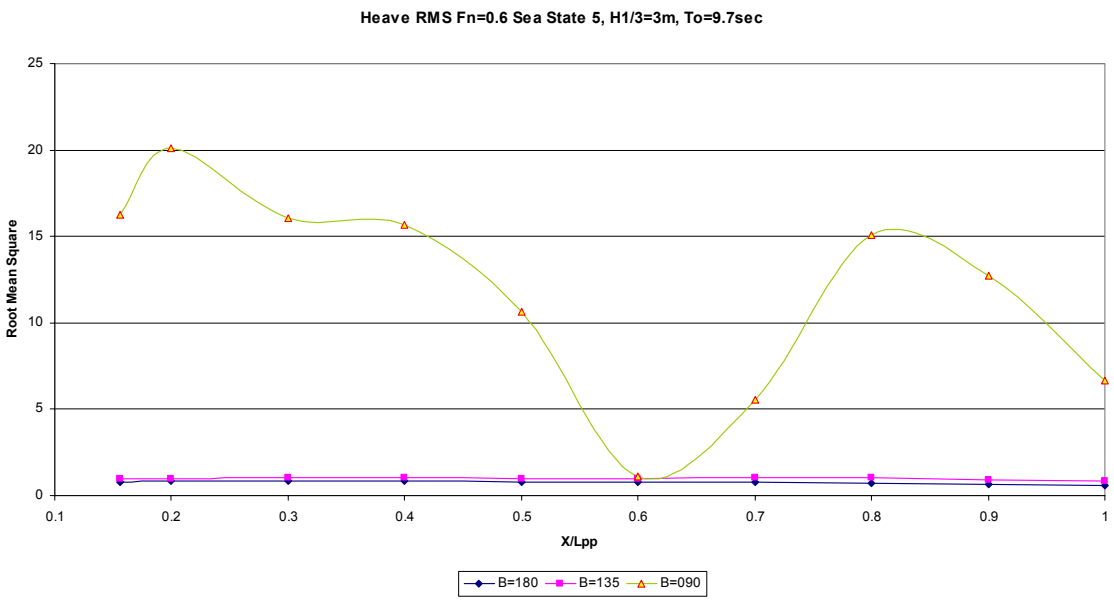

Figure 54. Fn=0.6 Heave RMS Values at Sea State 5 for Different Headings

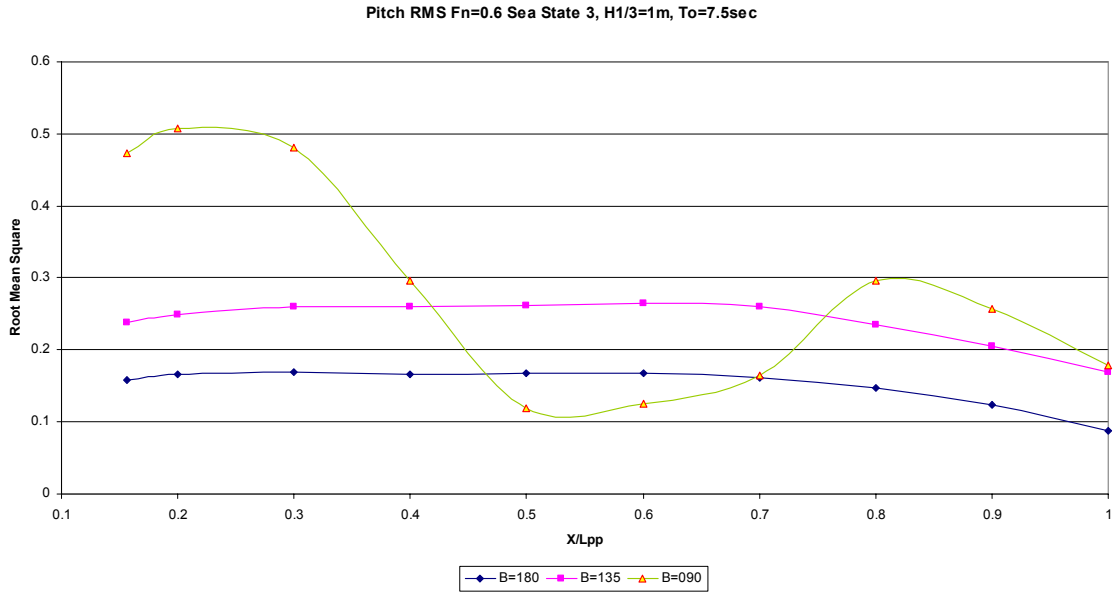

Figure 55. Fn=0.6 Pitch RMS Values at Sea State 3 for Different Headings

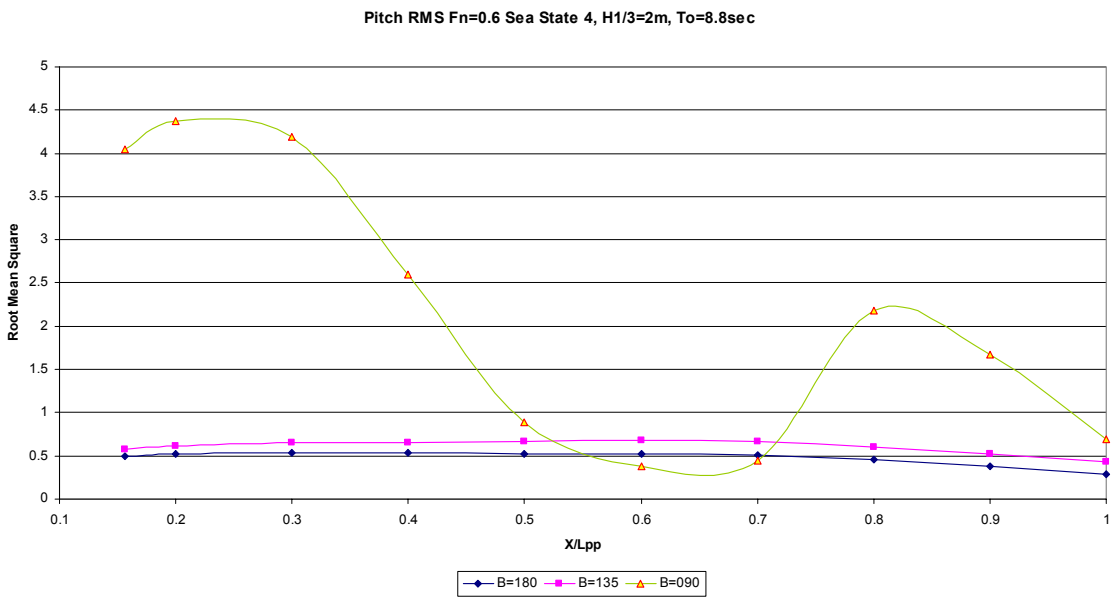

Figure 56. Fn=0.6 Pitch RMS Values at Sea State 4 for Different Headings

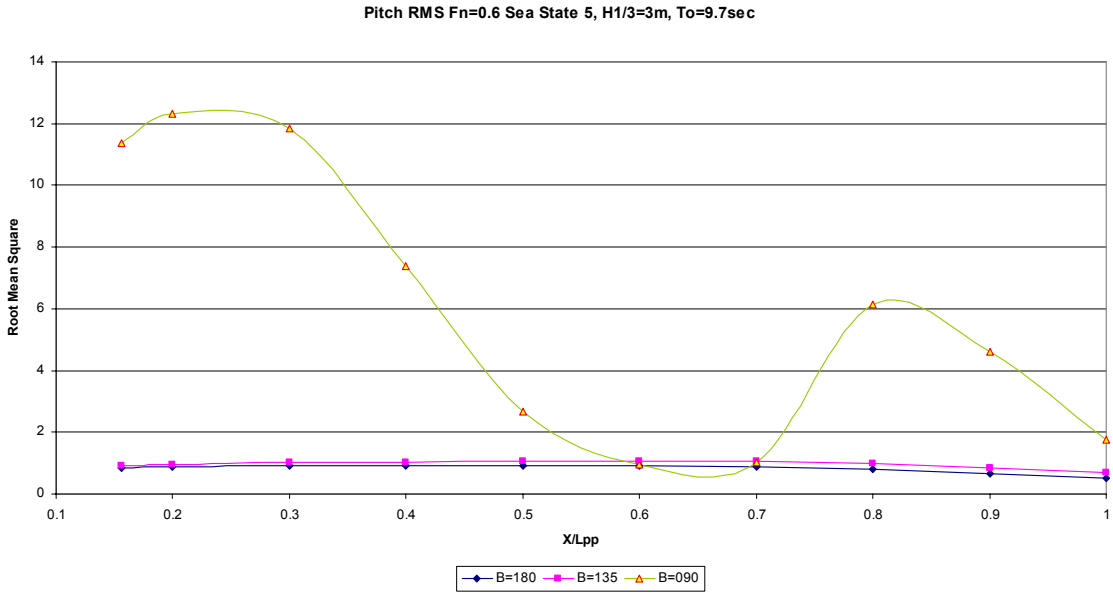

Figure 57. Fn=0.6 Pitch RMS Values at Sea State 5 for Different Headings

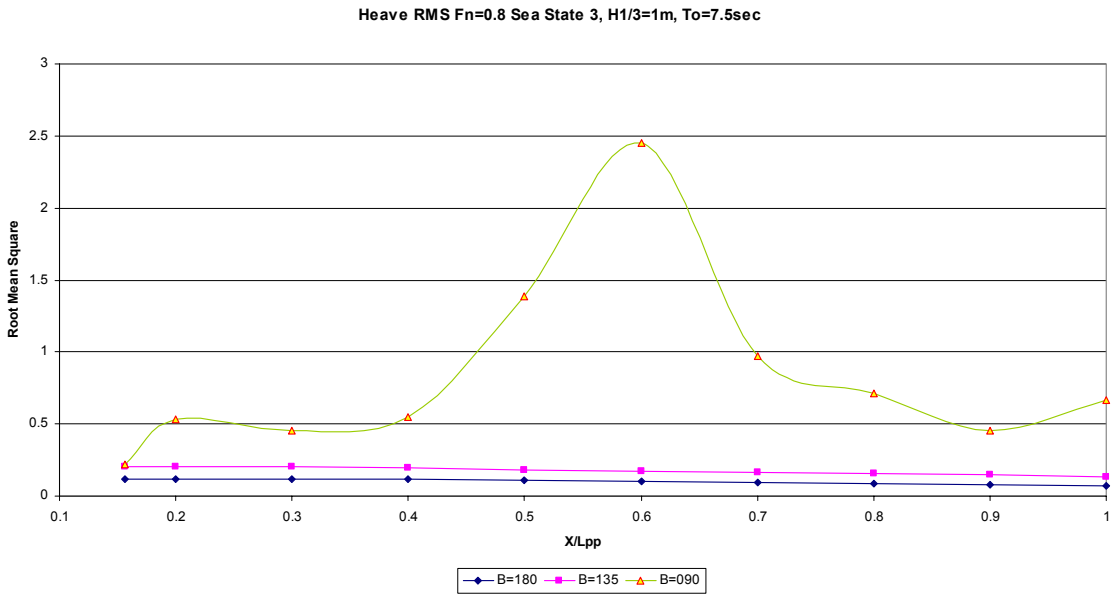

Figure 58. Fn=0.8 Heave RMS Values at Sea State 3 for Different Headings

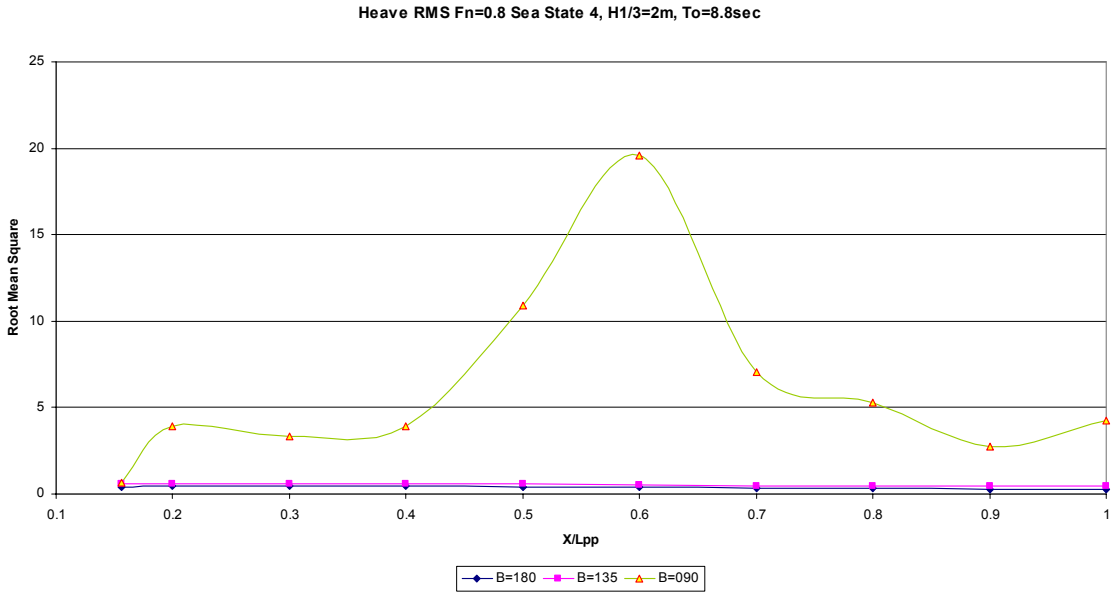

Figure 59. Fn=0.8 Heave RMS Values at Sea State 4 for Different Headings

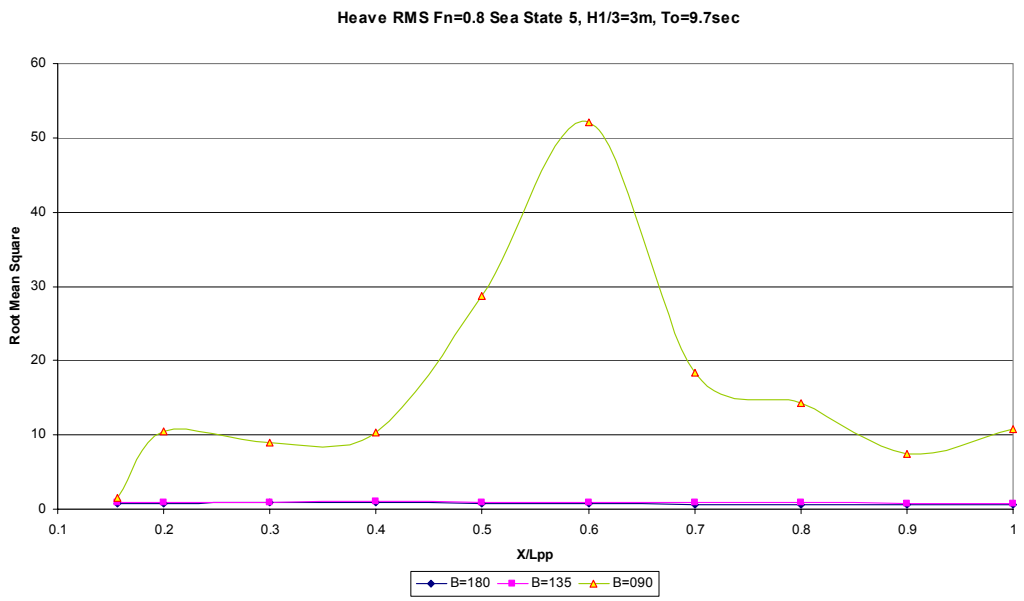

Figure 60. Fn=0.8 Heave RMS Values at Sea State 5 for Different Headings

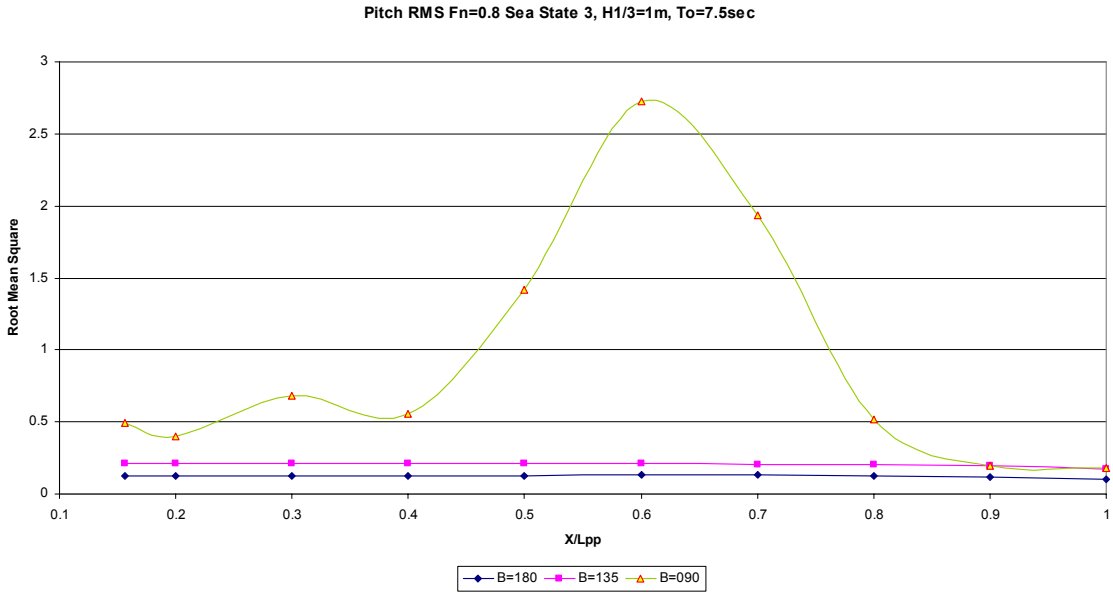

Figure 61. Fn=0.8 Pitch RMS Values at Sea State 3 for Different Headings

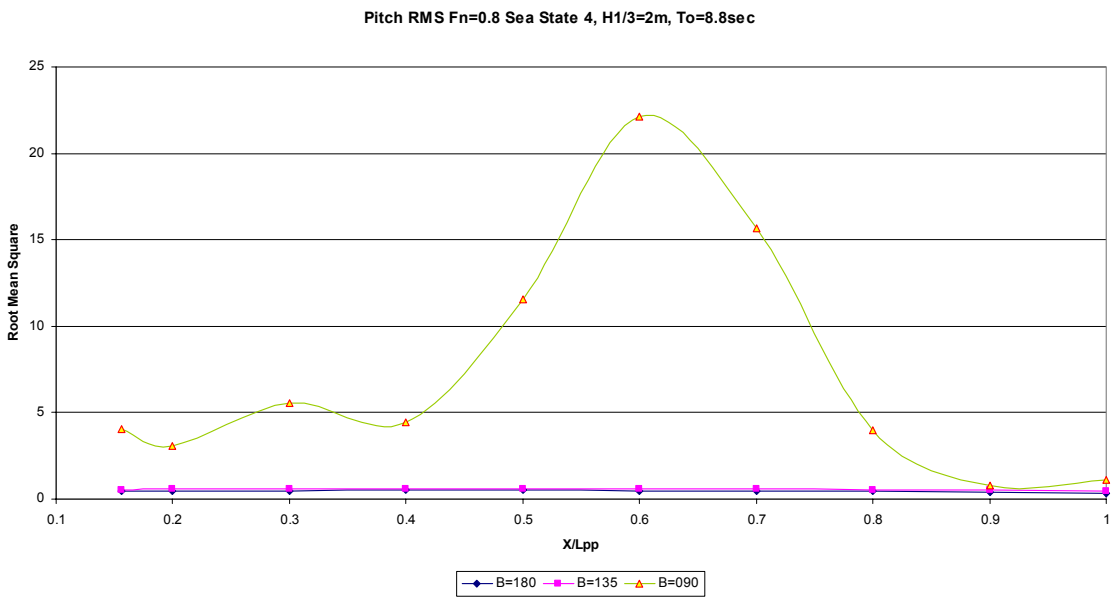

Figure 62. Fn=0.8 Pitch RMS Values at Sea State 4 for Different Headings

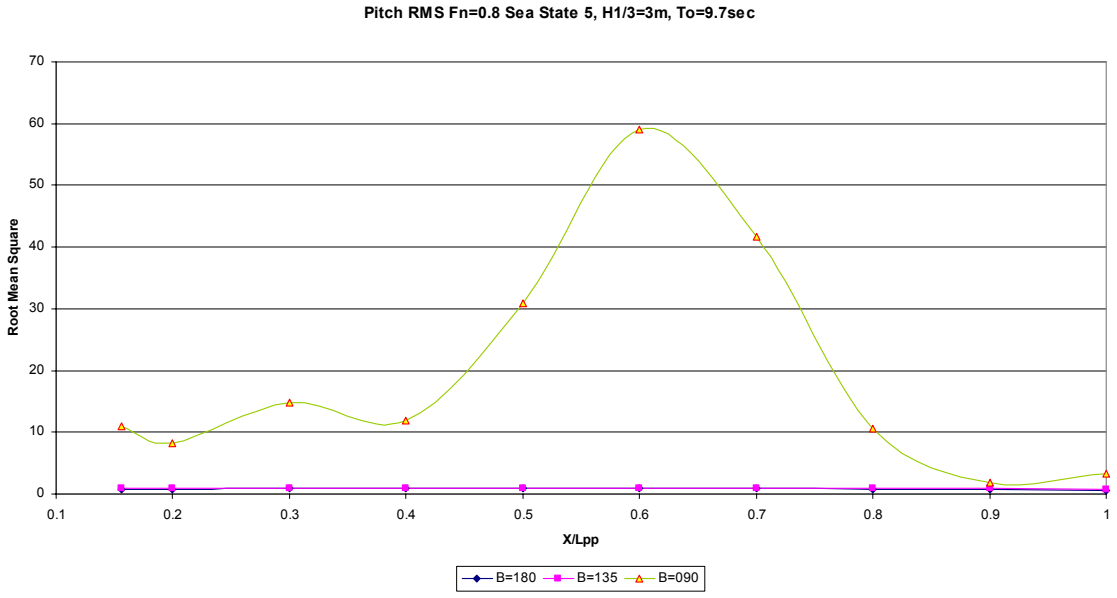

Figure 63. Fn=0.8 Pitch RMS Values at Sea State 5 for Different Headings

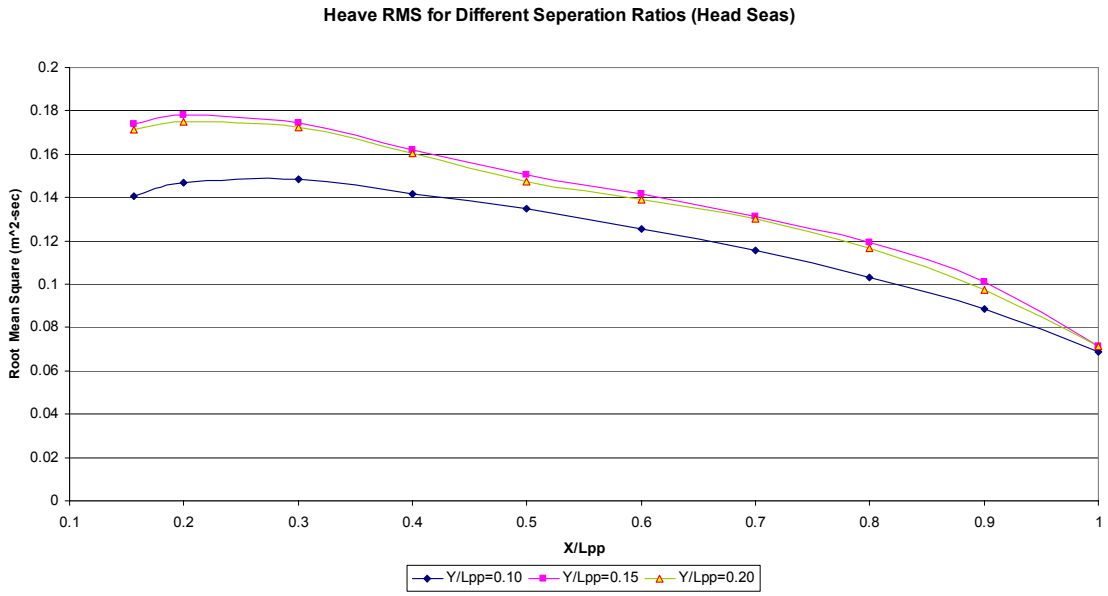

Figure 64. Heave RMS Values at Different Separation Ratios for Head Seas

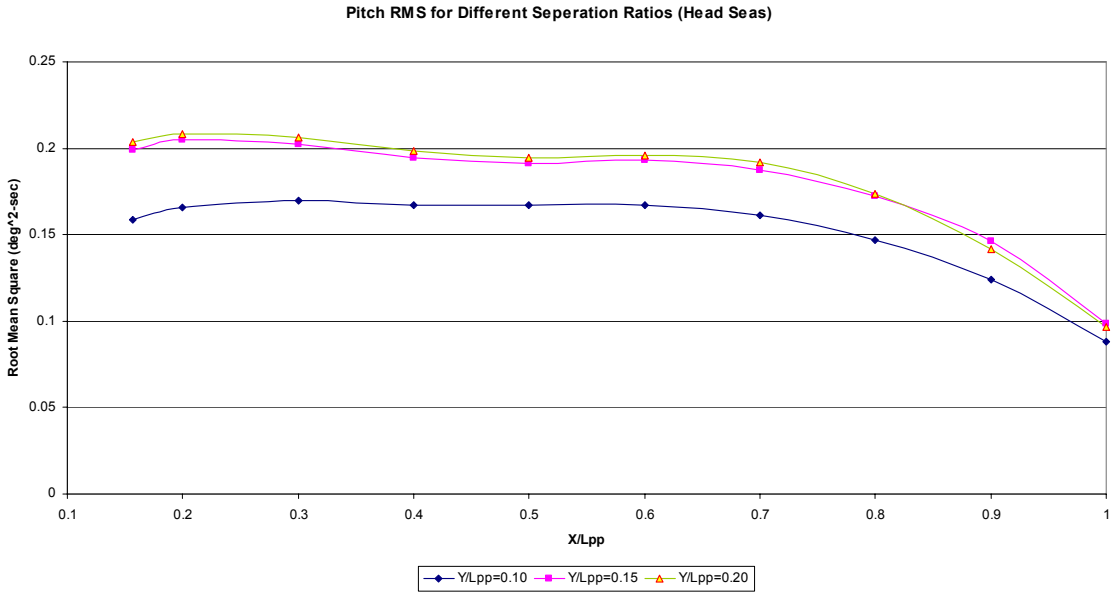

Figure 65. Pitch RMS Values at Different Separation Ratios for Head Seas

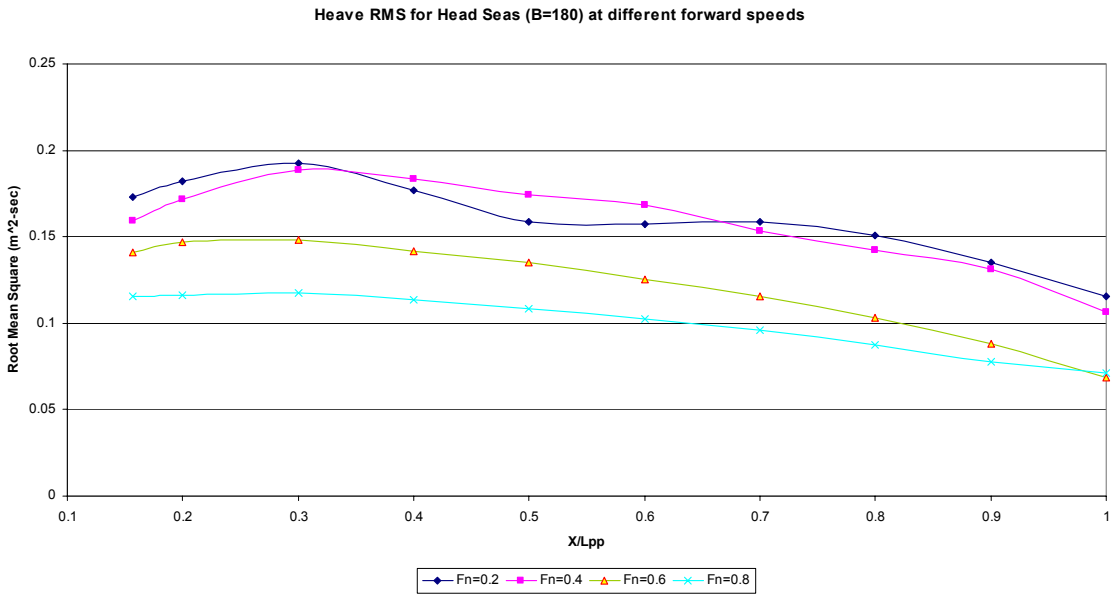

Figure 66. Heave RMS Values at Different Forward Speeds for Head Seas

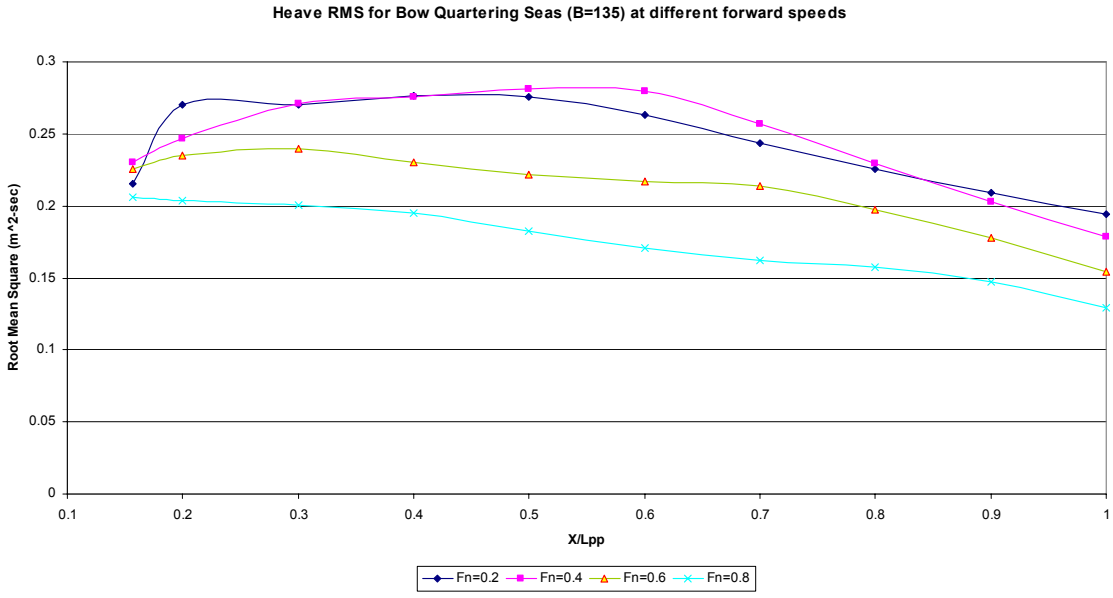

Figure 67. Heave RMS Values at Different Forward Speeds for Bow Quartering Waves

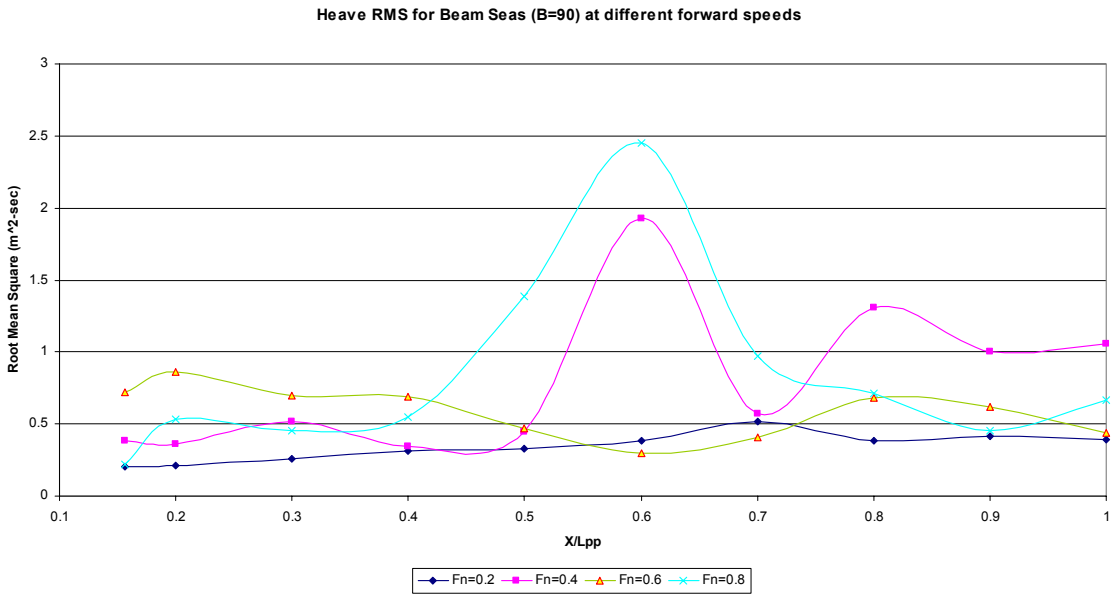

Figure 68. Heave RMS Values at Different Forward Speeds for Beam Waves

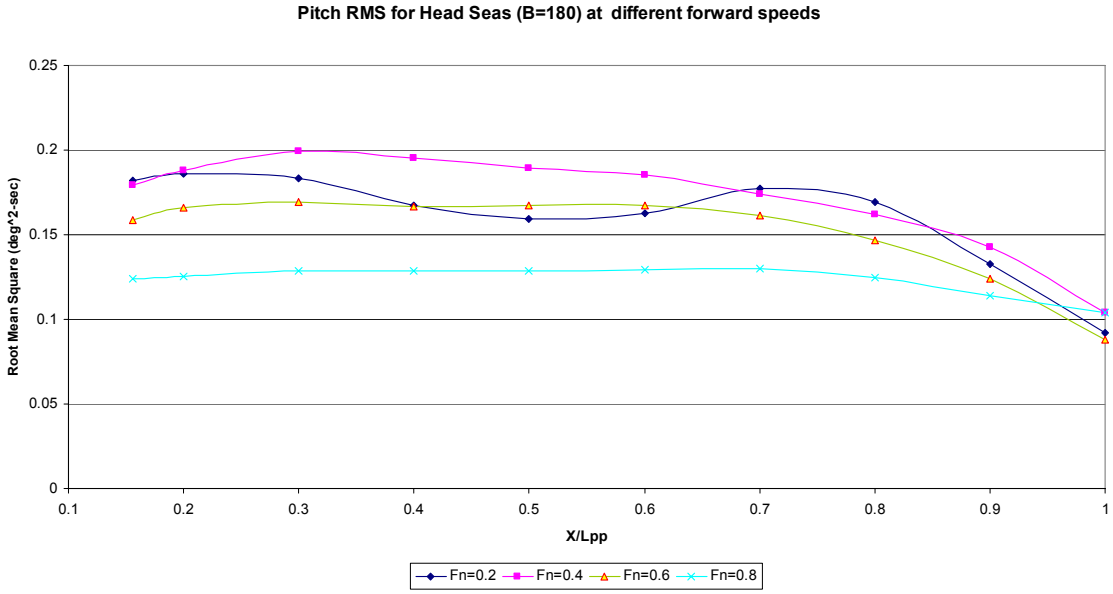

Figure 69. Pitch RMS Values at Different Forward Speeds for Head Seas

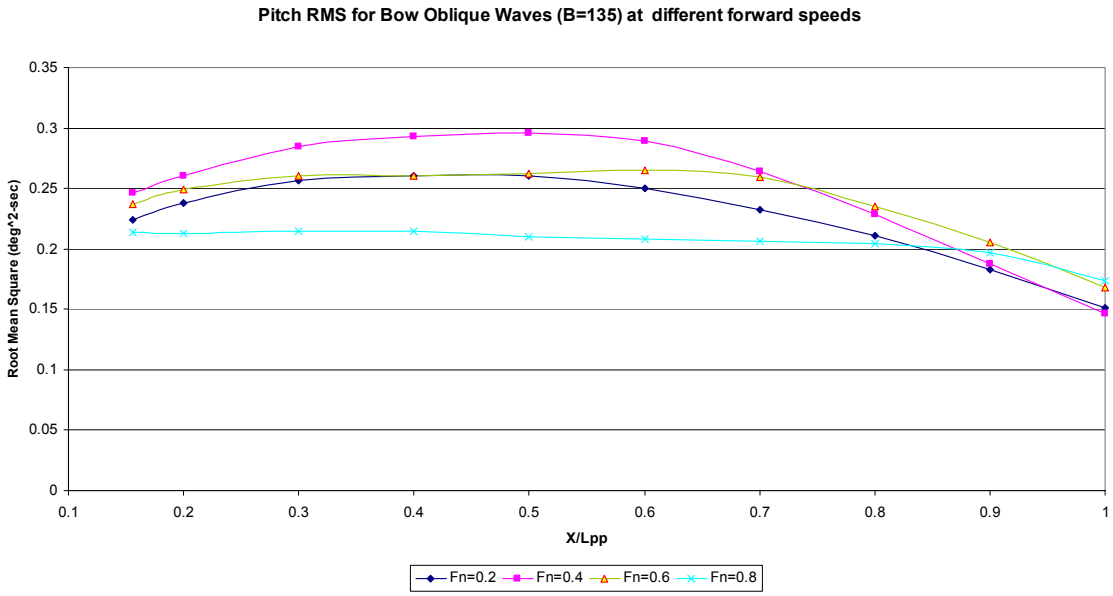

Figure 70. Pitch RMS Values at Different Forward Speeds for Bow Quartering Waves

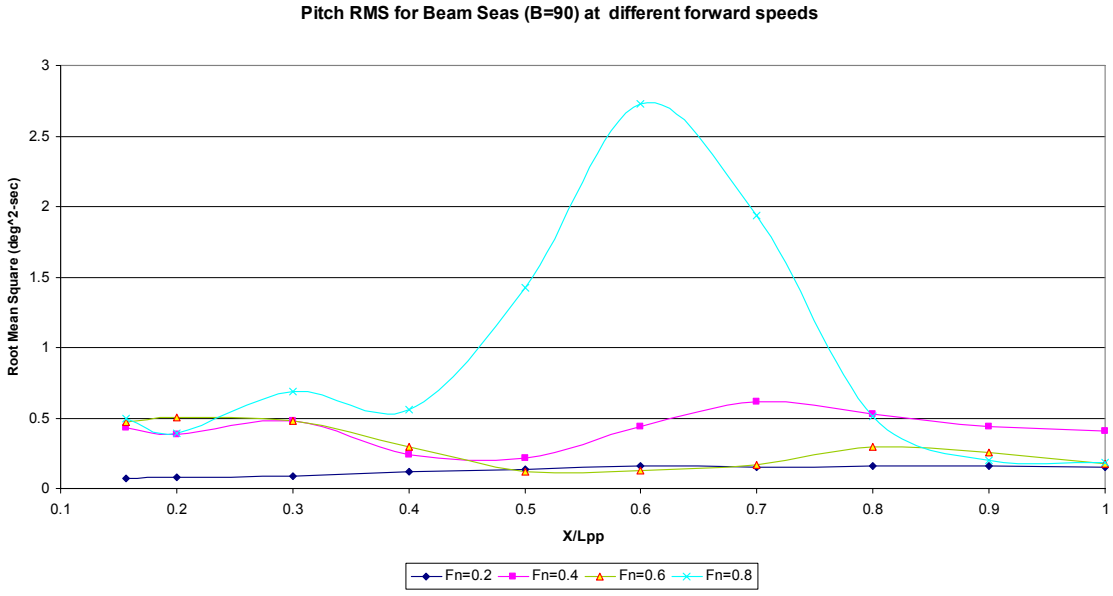

Figure 71. Pitch RMS Values at Different Forward Speeds for Beam Waves

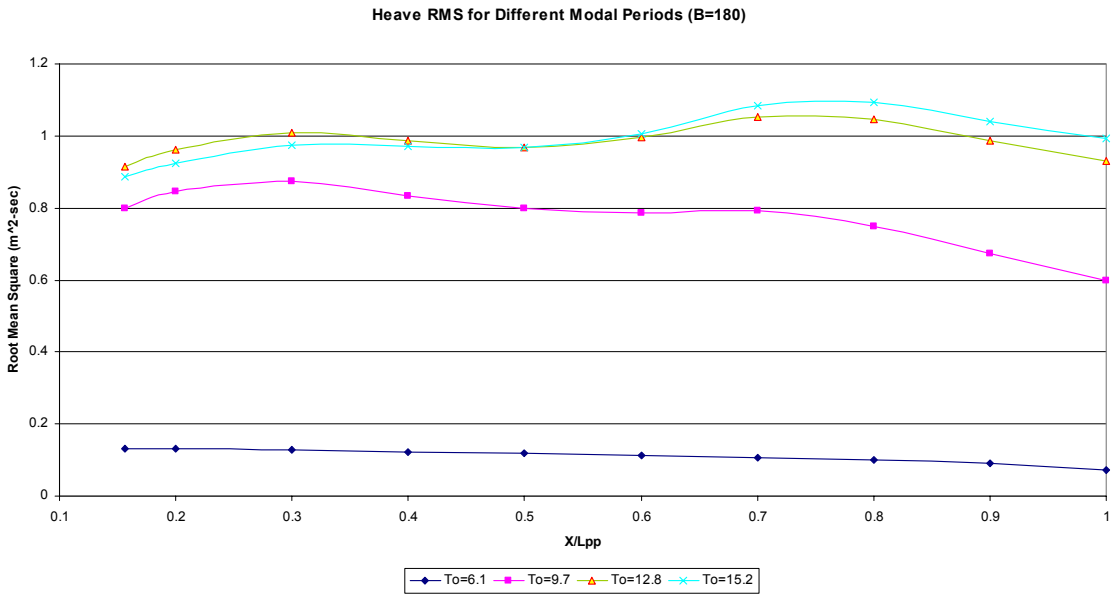

Figure 72. Heave RMS Values at Different Modal Periods for Head Seas

VI. CONCLUSIONS AND RECOMMENDATIONS

A. CONCLUSIONS

The main conclusions from this research can be summarized as follows:

1. There is no consistent trend for side hull placement in terms of the ship's seakeeping performance, for all forward speeds, sea directions, and modal periods.
2. In general, for heave and pitch motions, seakeeping behavior favors fore or aft placement of the side hulls.
3. Lower side-to-main hull separation results in better seakeeping characteristics, especially for head seas.

B. RECOMMENDATIONS

Some recommendations for further research are as follows:

1. Perform a sensitivity analysis in terms of the relative length and various drafts of the side hulls.
2. Analyze the seakeeping response in terms of horizontal plane motions.

THIS PAGE INTENTIONALLY LEFT BLANK

LIST OF REFERENCES

[1] *Littoral Combat Ship.* [editorial] URL: http://www.globalsecurity.org/military/systems/ship/lcs.htm. Accessed July, 2003.

[2] Broadbent C, Kennell C. *Monohull, Catamaran, Trimaran & SES High Speed Sealift Vessels.* Presented at 6th International Conference on Fast Sea Transportation (FAST 01). Naval Surface Warfare Center, Carderock Division. September, 2001.

[3] Lamb GR. *High Speed Sealift Technology Development Plan.* Total Ship Systems Engineering Directorate Technology Projection Report, NSWCCD-20-TR-2002/06. Bethesda, MD. May, 2002.

[4] Foxwell D, Scott R. *Advanced hullforms break the conventional mould*. Jane's Navy International 2003 April 01.

[5] Schmidt TW. *SLICE: A Revolutionary New Ship*. United States Japan Natural Resources/Marine Facilities Panel. Tokyo, Japan. May 17, 2000.

[6] *Skjold Class Missile Fast Patrol Boats*. URL: http://www.naval-technology.com/projects/skjold/index.html. Accessed October, 2003.

[7] Griethuysen WJ, Bucknall RWG, Zhang JW. *Trimaran Design-Choices and Variats for Surface Warship Applications.* Presented at Warship 2001, Future Surface Warships, London. 20 & 21 June 2001.

[8] Wilson J. *Sea Power 2000*. Popular Mechanics [serial online] URL: http://www.popularmechanics.com/science/military/1999/11/sea_power_2000/. Accessed October, 2003.

[9] Helasharju H, Sundell T, Rintala S, Karppinen T. *Resistance and Seakeeping Characteristics of Fast and Large Multihull Vessels.* Presented at the Third International Conference on Fast Sea Transportation (FAST 95). Lubeck-Travemunde, September, 1995.

[10] Preston A. *Sea Power International, Rolls-Royce Estabishes U.S.-Oriented Naval Facility.* Navy League of the U.S. [serial online] URL: http://www.navyleague.org/seapower_mag/july2001/sea_power_international.htm. Accessed September, 2003.

[11] Sclavounos PD, Purvin S, Ulusoy T, Kim S. *Simulation Based Resistance and Seakeeping Performance of High Speed Monohull and Multihull Vessels Equipped with Motion Control Lifting Appendages.* Keynote Lecture. Seventh International Conference on Fast Sea Transportation (FAST 2003). Ischia, Italy. October, 2003.

[12] Sclavounos PD. *Computation of Wave Ship Interactions.* In M. Ohkusu, Editor, Computational Mechanics Publications, 1996.

[13] Dawson. *A Practical Computer Program for Solving Ship-Wave Problems.* Proceedings Second International Conference on Numerical Ship Hydrodynamics. Berkeley, CA 1977.

[14] Beck RF, Reed AM. *Modern Computational Methods for Ships in a Seaway.* Presented at Twenty-Third Symposium on Naval Hydrodynamics. Val de Reuil, France. September, 2000.

[15] Sclavounos PD, Nakos D. *Ship Motions by a Three-Dimensional Rankine Panel Method.* Presented at Eighteenth Symposium on Naval Hydrodynamics. The Univercity of Michigan, Ann Arbor. August, 2001.

[16] Papoulias FA. *Ship Dynamics.* TS4001: Integration of Naval Engineering Systems Lecture Notes. URL: http://web.nps.navy.mil/~me/tsse/TS4001/support/1-11-1.pdf. Accessed March, 2003.

[17] Lewis EV. *Principles of Naval Architecture*, *The Motion of Ships in Waves, Chapter IX*. New York; The Society of Naval Architects and Marine Engineers; 1967. 827 p.

[18] Lloyd ARJM. *Seakeeping: Ship Behavior in Rough Weather.* West Yorkshire; Ellis Horwood Ltd; 1989. 395 p.

[19] Zubaly RB. *Applied Naval Architecture.* Maryland; Cornell Maritime Press; 1996. 349 p.

[20] McCreight KK. *A Note on the Selection of Wave Spectra for Design Evaluation.* Hydromechanics Directorate Research and Development Report, Naval Surface Warfare Center, Carderock Division. Bethesda, MD. January, 1998.

[21] *SWAN2 2002: Ship Flow Simulation in Calm Water and in Waves: User Manual.* Boston Marine Consulting Inc.

THIS PAGE INTENTIONALLY LEFT BLANK

INITIAL DISTRIBUTION LIST

1. Defense Technical Information Center
   Ft. Belvoir, Virginia

2. Dudley Knox Library
   Naval Postgraduate School
   Monterey, California

3. Mechanical Engineering Department Chairman, Code ME
   Naval Postgraduate School
   Monterey, California

4. Naval Mechanical Engineering Curriculum Code 34
   Naval Postgraduate School
   Monterey, California

5. Professor Fotis Papoulias, Code ME
   Department of Mechanical Engineering
   Naval Postgraduate School
   Monterey, California

6. Deniz Kuvvetleri Komutanligi
   Personel Daire Baskanligi
   Bakanliklar, Ankara, TK

7. LTJG Aziz Alper Kurultay
   Deniz Abdal Mah. Cesme Sokak
   No: 31 Daire: 5 Capa
   34280 Istanbul, TK